Pergamon

PII: S0743-9547(96)00081-5

Journal of Asian Earth Sciences, Vol. 15, No. 1, pp. 61–88, 1997

1367-9120/97 $17.00 + 0.00

Neogene basin history and paleomagnetism of a rifted and inverted forearc region, on- and offshore Sumba, Eastern Indonesia

A. R. Fortuin,* W. Van der Werff†‡ and H. Wensink§

*Centre of Marine Earth Sciences, Vrije Universiteit, De Boelelaan 1085, 1081 HV Amsterdam, The Netherlands;

†Netherlands Institute for Sea Research, P.O. Box 59, 1790 AB Den Burg, Texel, The Netherlands;

§Paleomagnetic Laboratory Fort Hoofddijk, University of Utrecht, Budapestlaan 17, 3584 CD Utrecht, The Netherlands

(*Received* 10 *December 1995; accepted for publication* 11 *December 1996*)

Abstract-The island of Sumba is located in the arc/trench gap at the junction of the Sunda and Banda Arcs. To elucidate its enigmatic forearc position, stratigraphic and paleomagnetic data were collected along three transects in central and east Sumba. Sumba represents the emerged part of a terrane of SE Asian origin. Results of stratigraphic and paleomagnetic investigations on central and east Sumba are presented and discussed in order to identify patterns of horizontal and vertical crustal movements. A synthetic seismogram of the onshore record enables correlation with the offshore Neogene E of Sumba, in order to interpret the data in a regional context.

The Neogene basin history of Sumba started when overall subsidence took place around the transition from Early to Middle Miocene. On east Sumba, above a basal condensed interval, up to 600 m of Middle-Late Miocene volcaniclastic submarine fan deposits occur. The sediments reflect island arc volcanism and are interpreted as parts of a prograding submarine fan system on a north-dipping paleoslope, fed by a volcanic source to the south of Sumba. Biostratigraphic data indicate a high volcanic supply during the middle Miocene and early-middle Tortonian, a waning supply during the late Tortonian and renewed supply during the Messinian. These patterns probably reflect variation in volcanic activity. During the Messinian calcilutites and foraminiferal chalks became dominant and deposition of these pelagic sediments continued into the Early Pliocene. Using the pattern of magnetic polarity, changes in a selected interval the position of the Miocene–Pliocene boundary is better constrained.

Seismic studies in the offshore area E of Sumba (Van der Werff 1995a, b) indicate the presence of an extensive tract of N-prograding turbidites on Sumba Ridge (Savu Basin). The proposed correlation with the onshore record suggests lateral continuity from the island into the offshore area, where the volcaniclastic submarine fan system presumably had its largest development,

Subsidence proceeded so fast (~ 1 m/ka) on east Sumba, that before the beginning of the Late Miocene, sediments were deposited below the CCD. This pattern suggests that the Sumba region underwent strong crustal attenuation due to rifting. As this was coupled with the arrival of volcaniclastics we envisage intra-arc rifting, coupled with the growth of a short lived volcanic arc further south. Its initiation at the transition of Middle-Late Miocene suggests interaction with the then approaching Banda Arc subduction system. The paleomagnetic data indicate that during this process Sumba was at a paleolatitude of ~ 12 ° South and underwent a counter-clockwise rotation of 5

The reappearance of planktonic foraminiferal assemblages during the latest Miocene and their present elevation above sea level suggest an average rate of post-Miocene uplift of ~ 0.7 mm/a. Emergence of Sumba probably did not take place before 3 Ma. This inverted motion of the Sumba terrane is probably coupled with the change to the present tectonic situation, in which volcanic activity was resumed in the present inner arc after a non volcanic interval during the spreading stage. © 1997 Elsevier Science Ltd

Introduction

The Indonesian island of Sumba is located at the junction of the Sunda Arc oceanic subduction system and the Banda Arc, where Australian continental crust becomes involved in the collision process (Fig. 1). Sumba is the emerged part of a larger, approximately WNW-ESE oriented forearc uplift at the junction of the Lombok and Savu forearc basins. This Sumba Ridge (Van Weering et al. 1989, 1994a) (Fig. 13) extends from the easternmost part of the Lombok Basin at 118°, into the Savu Basin until 121°30′, where it borders the Savu thrust zone. South of Sumba (near 120"E) the more than 6 km deep Java Trench of the Sunda subduction front shallows rapidly, curves southward, and passes into a more diffuse plate boundary where the Australian continental crust becomes involved. Here, the up to 3 km deep Timor Trough is its clearest expression (Harris 1991; Masson et al. 1991). Recently obtained geophysical data (Genrich et *al.* 1996; Snyder et *al.* 1996) indicate that much of the present northward motion of Australia

‡Present address: Geological Survey of Japan, l-l-3 Higashi, Tsukuba, Ibaraki, 305 Japan.

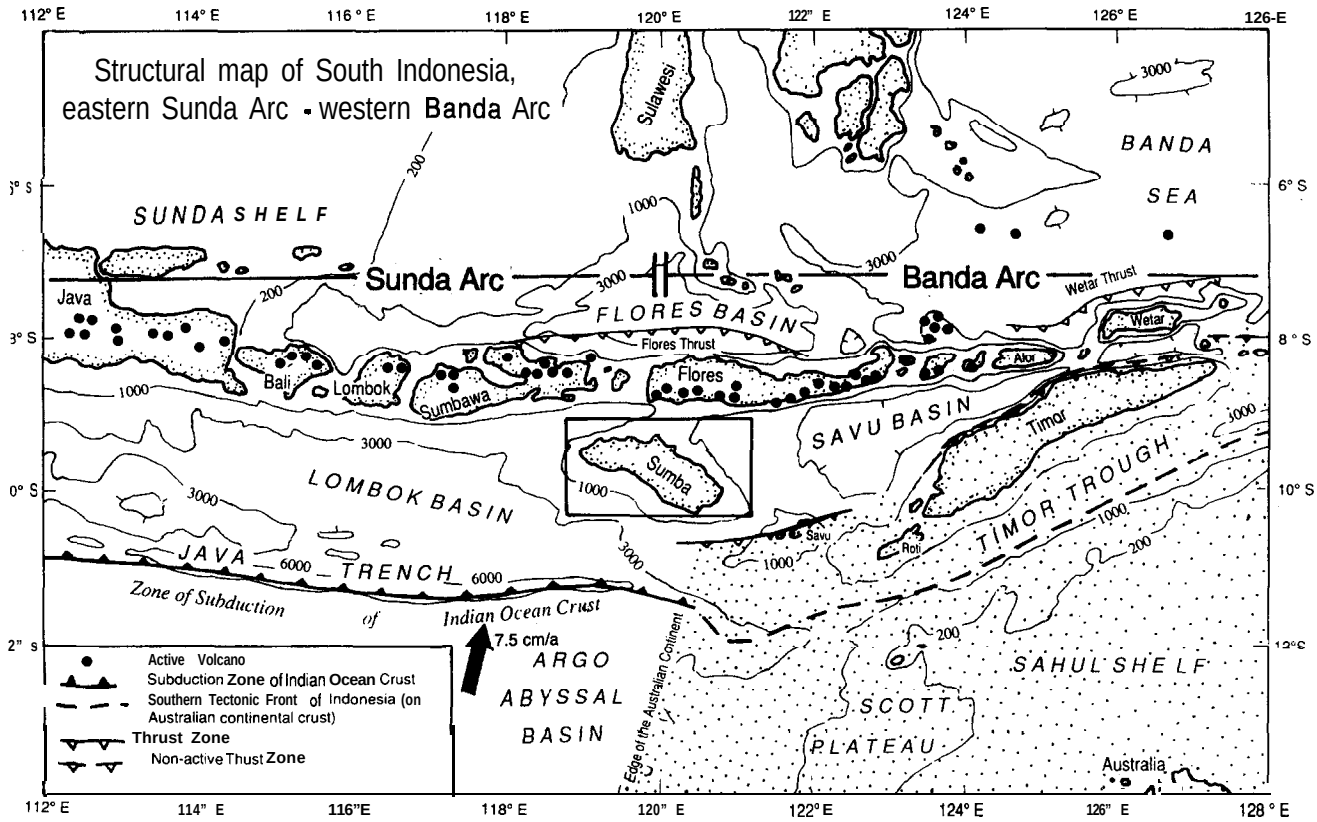

Fig. 1. Map of central southern Indonesia showing the position of Sumba at the eastern end of the Sunda Arc. The dotted area indicates the outline of the Australian continental crust. The arrow indicates the direction and estimated rate of convergence between Australia and Eurasia at the Timor Trough (after DeMets *et al. 1990).*

relative to Eurasia occurs N of Timor, along the Flores and Wetar thrust zones (Fig. 1). Moreover, these findings confirm older interpretations (Audley Charles 1975) that Sumba is situated in a transition zone between the inner eastern Sunda Arc and the southern Banda Arc area. Genrich *et al.* (1996) measured considerable change in the motion relative to the Sunda shelf between the Sumba and Banda segments, which is ~ 20 cm/yr on Sumba and W. Flores and ~ 60 cm/yr at eastern Flores. This differential crustal motion causes sinistral shear in a zone more or less conforming to the edge of the subducted continental shelf of Australia and extending towards Flores.

Sumba is generally regarded as a micro-continent. Until recently its possible provenance from either Australia, southeast Asia, or an intra-Tethys position remained a matter of controversy. Recent paleomagnetic and isotope studies (Wensink 1994; Wensink and Van Bergen 1995; Vroon 1996), however, confirm Sumba's affinity with southeast Sundaland, as earlier suggested by Hamilton (1979). According to Wensink (1994) the Sumba terrane drifted from a slightly more northern position along the Southeast Asian margin and became trapped in a forearc basin setting in the late Oligocene (Hamilton 1979; Chamalaun *et al.* 1982). Despite its position at the western boundary of the collision zone between the Banda Arc and Australia, the deformation of Sumba since the Middle Miocene is mild and characterized by gentle overall tilting in a northward direction, of the widely exposed upper Cenozoic sediments (Fig. 2A).

The purpose of this paper is to present geological data obtained from an investigation of Neogene sedimentary record of Sumba, in order to arrive at a model of its geological evolution since the Miocene. In a previous paper (Fortuin *et al.* 1994) our first stratigraphical results were presented. To our surprise, we then had to conclude that the volcaniclastic turbidites, characterizing the deep water sediments presently exposed on east Sumba, were supplied by sources to the south of the island, rather than from the volcanic edifices towering above the inner arc islands of Sumbawa and Flores to the north of Sumba (Fig. 1). This showed us that little is known about the paleogeographic evolution of this region. In order to view the Neogene history of Sumba in a regional perspective, it was decided to present the geological results from three points of view:

Fig. 2. Maps of Sumba Island. Fig. 2A shows the main morpho-tectonic units, topographic names and 1000 m isobaths. The position of Transects I-III and seismic profile Pac-109 are indicated. The heavy line of the latter profile marks the seismic profile reproduced in Fig. IO. Map B shows East Sumba giving the main drainage pattern, the location of the stratigraphic sections (numbered localities) and the paleomagnetic sampling sites (SS codes). F1 indicates the approximate position of a concealed NE-SW basement fault. F2 and F3 indicate offshore basement faults. For E Sumba the 500 and 1000 m contours are given (these data not available for central Sumba).

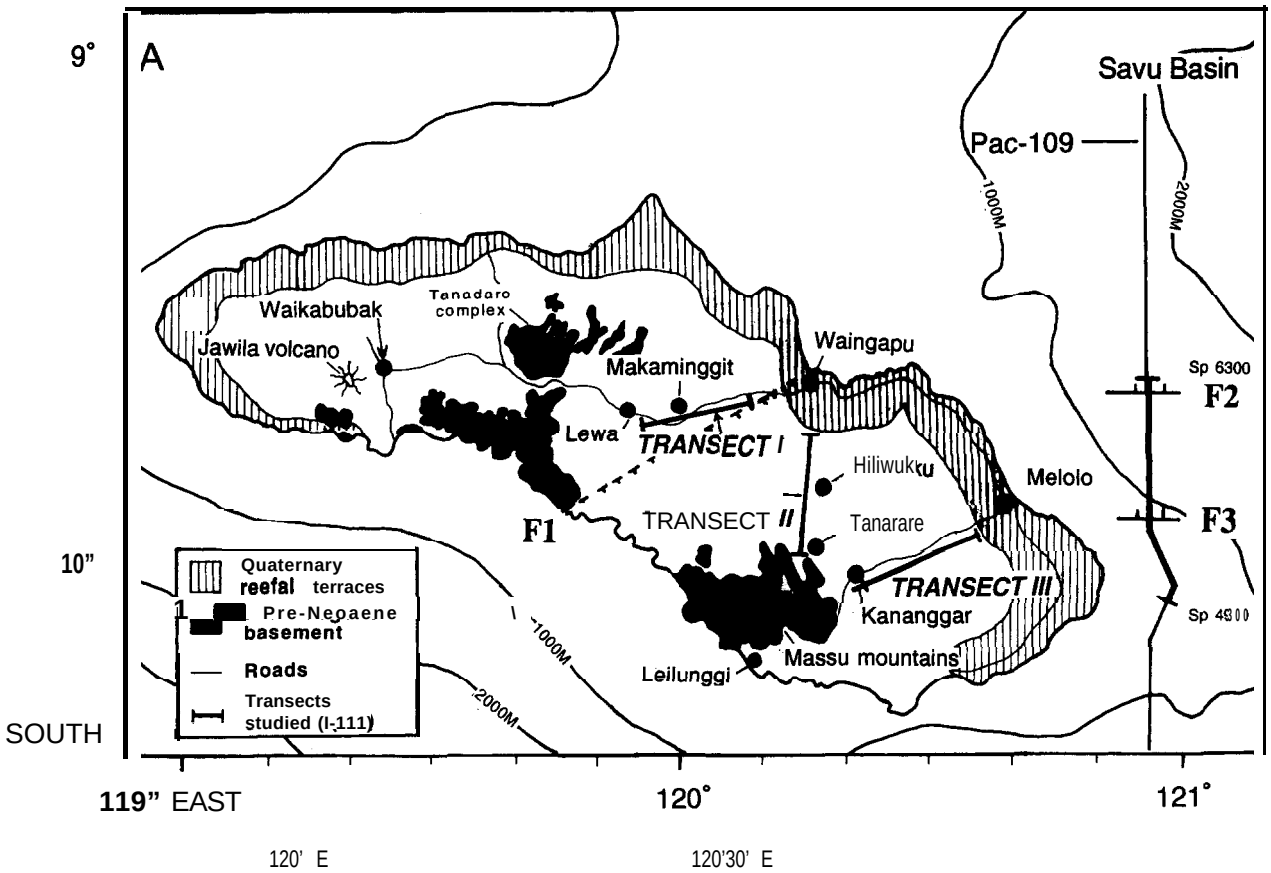

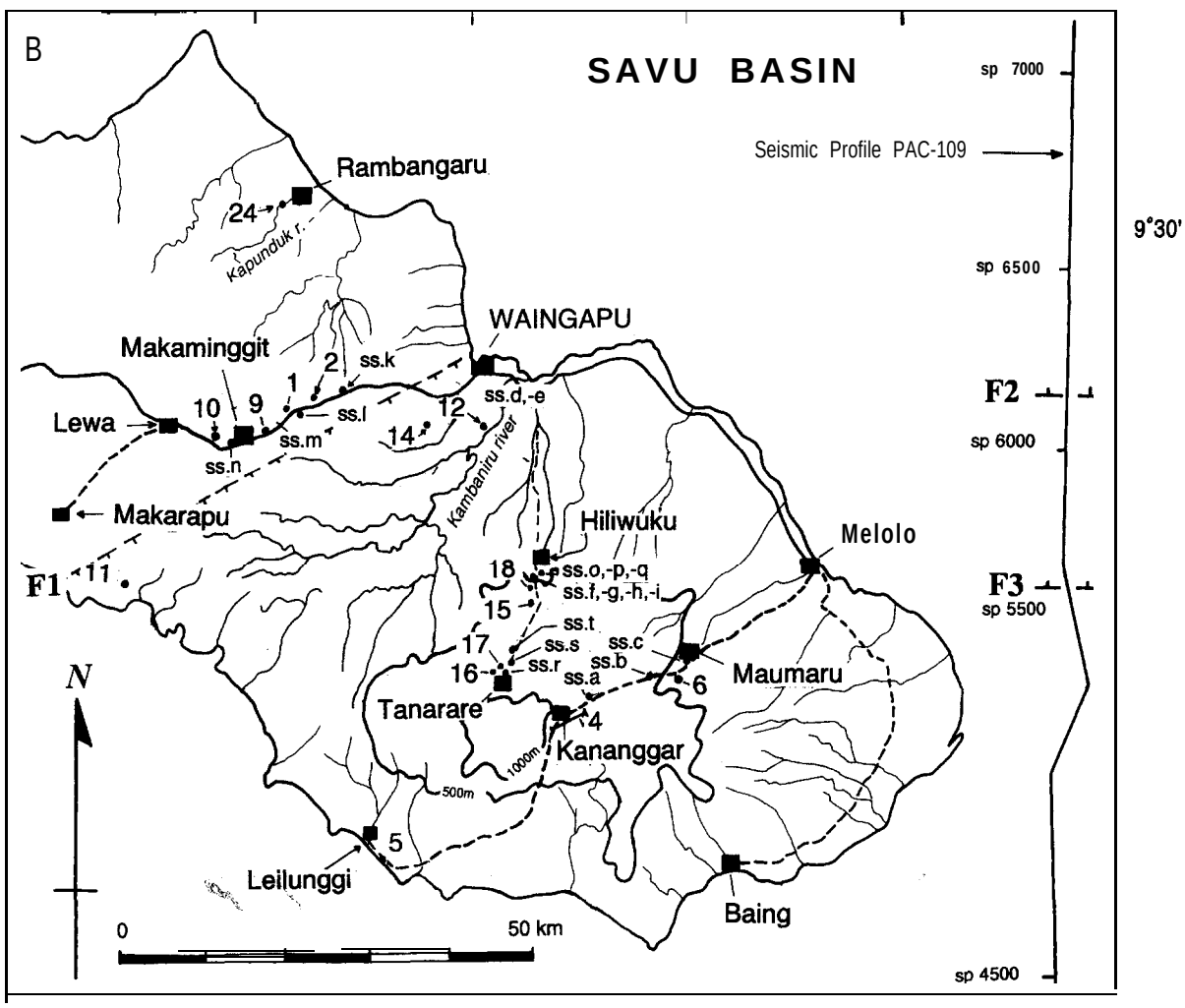

Figure 2A and B.

First, the sedimentary data are given, as obtained from the study of 3 transects across central and eastern Sumba (Fig. 2A). Secondly, paleomagnetic aspects are discussed. Previous paleomagnetic studies of Sumba (Otofuji *et al.* 1981; Chamalaun and Sunata 1982; Wensink 1994; Wensink and Van Bergen 1995) aimed to elucidate the late Cretaceous through late Eocene motion history. The present studies are included to constrain: (a) possible late Neogene motion and/or rotation after the complex mise-en-place of the Sumba terrane at the extreme southeast Asian continental margin and, (b) biostratigraphic problems regarding the position of the Miocene-Pliocene boundary. The third aspect concerns correlation of the onshore record with the main seismic facies units of the Savu Basin to the east (Fig. 1), using a synthetic seismogram of the Neogene of transect II (Fig. 2A). Seismo-stratigraphic studies of the Lombok and Savu basins reveal the general outline of the Cenozoic history of these forearc basins (Van Weering *et al.* 1989; Van der Werff *et al.* 1994a, b; Van der Werff 1995a), but lack of well data limits the "ground truthing" of regional plate-tectonic scenarios (Rangin *et* al. 1990; Daly *et al.* 1992; Hall 1996). The paper finally discusses the geohistorical aspects and regional plate tectonic changes.

Geological Setting

Although many data have been published concerning aspects of the various rock units in Sumba, a comprehensive structural and stratigraphic overview is still lacking. Aspects of the stratigraphy of Sumba have been discussed by Van Bemmelen (1949), Hamilton (1979), Chamalaun et al. (1982), Von der Borch *et al.* (I 983), Audley-Charles (1985), Fortuin *et al.* (1984) and Wensink (1994). The main stratigraphic and tectonic developments are as follows:

Pre-Neogene basement rocks are exposed in a number of structural highs on Sumba (Fig. 2A). They underwent several episodes of block faulting and only minor folding before deposition of the Neogene (Burollet and Sallé 1982). The oldest sediments are of Cretaceous age-open marine shales, tuffaceous sandstones, diamictites and turbidites-occurring mainly in W. Sumba (Lasipu Formation). In SE Sumba shallow marine siltstones and sandstones including volcaniclastic interbeds occur (Veenhof 1990). Samples investigated contain middle Cretaceous dinoflagellate assemblages suggesting a north Tethys affinity (W. Herngreen, pers. comm.). Widespread igneous and volcanic activity took place during both the late Cretaceous and Paleogene. Shallow marine platform carbonates and associated facies of Eocene to early Miocene age developed around the gradually subsiding eruption centres (Paumbapa Formation). Early Miocene volcanic activity has been reported for W. Sumba (Jawila Formation, Effendi and Apandi 1981; Wensink and Van Bergen 1995). These deposits consist of up to 300 m thick volcanic diamictites, andesitic lavas and locally intercalated coral reef build-ups, and/or continental strata including silicified logs. A recently dated andesite however, suggests a late Ecocene age.

The main orientation of the faults is NE–SW and WNW-ESE (Veenhof 1990). Reactivation of fault blocks occurred during and after the late Miocene with consistent downthrow to the south and north of a core of maximum uplift, located along the Massu mountains and its eastern offshore continuation, the Sumba Ridge. These uplifts and their unconformably overlying Neogene cover are slightly tilted to the north.

The middle Miocene to early Pliocene deposits are up to 600 m thick. They were named the Sumba Formation (Van Bemmelen 1949), but Effendi and Apandi (198 1) made a division into the Waikabubak and Kananggar formation in order to distinguish the chalky and volcaniclastic facies. All over western and central Sumba reefal limestones and chalks of the Waikabubak Formation are recognized, whereas east of a poorly constrained fault zone (F1, Figs 2A, B), where the amount of intercalated volcaniclastic turbidites, debris flows and slumps increases rapidly, the Kananggar Formation is widely exposed.

Due to Sumba's gradual late Cenozoic emergence, the margins of the island are covered by Quaternary reef terraces (Fig. 2A). These are very well developed along the north coast (Hantoro 1992). The highest terraces observed by the present team are at 600 m altitude. In the Waingapu area these reefal deposits interfinger with, and partly overlie up to over 100 m of coarse clastic fan delta deposits (Fortuin *et al.* 1994b). These latter authors report a faint tilting of the older flights of terraces.

Methods

The geological data are based on the study of 3 transects across central and east Sumba (Fig. 2), expanded with a number of isolated sections. For each transect a composite lithological column has been compiled (Fig. 3) using the information from lithologically correlated individual sections. Low strata1 dips and considerable lateral continuity of the facies units enabled reliable lithological correlations of the most relevant sections within one transect. Individual sections were given a number (Fig. 2B) and logged and measured using a hand held levelling instrument. Samples for biostratigraphic purposes were taken at 2–4 m intervals. In the lithological columns, pelitic and coarser intervals are indicated, but no distinction is made within the pelitic intervals between more chalky, clayey or tuffaceous varieties (except where pure chalky sediment predominates).

For the paleomagnetic research, oriented block samples were collected at 23 sites, all fresh road

Fig. 3. Lithostratigraphic columns of the Neogene of Transects I-III. In addition biozones and age correlations are given, based on planktonic foraminiferal and calcareous nannofossil data. Vertical scale in metres. In each transect column the position of the section numbers is at the base of that section. The planktonic foraminiferal zones (N) or nannofossil zones (NN) are indicated at the level where these could be certified for the first time. The WS numbers in Transect II indicate the position of the samples used for the petrophysical analysis (Table 4).

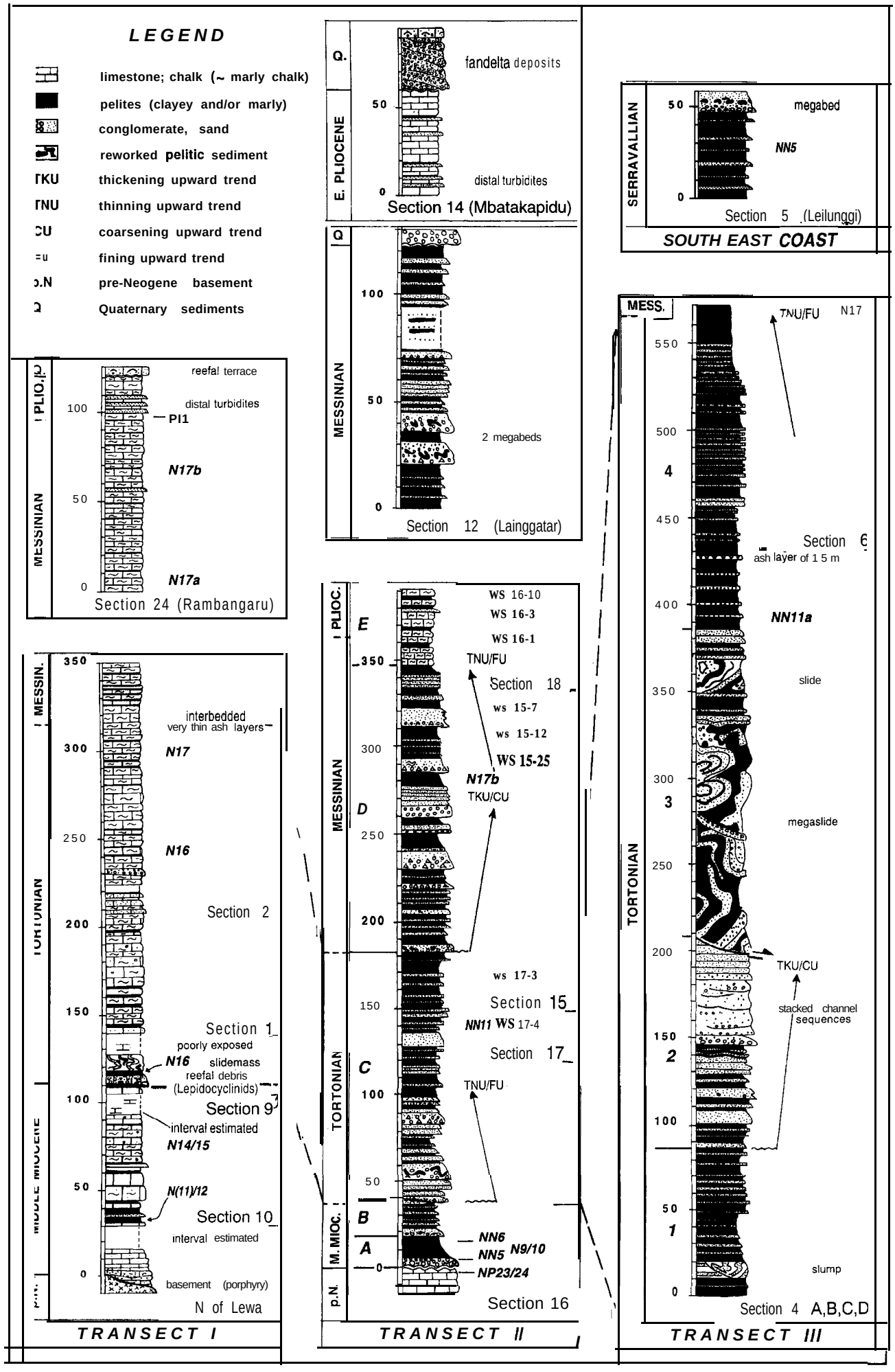
LEGEND
limestone; chalk (~ marly chalk)
pelites (clayey and/or marly)
conglomerate, sand
reworked pelitic sediment
TKU thickening upward trend
TNU thinning upward trend
CU coarsening upward trend
=u fining upward trend
p.N pre-Neogene basement
Q Quaternary sediments
Q.
E. PLIOCENE
fandelta deposits
distal turbidites
Section 14 (Mbatakapidu)
SERRAVALLIAN
megabed
NN5
Section 5 (Leilunggi)
SOUTH EAST COAST
Q
MESSINIAN
2 megabeds
Section 12 (Lainggatar)
reefal terrace
distal turbidites
PI1
N17b
N17a
Section 24 (Rambangaru)
MESS.
TNU/FU
N17
Section 6
ash layer of 1 5 m
NN11a
slide
megaslide
TKU/CU
stacked channel sequences
slump
Section 4 A,B,C,D
TRANSECT III
E
D
C
B
A
WS 16-10
WS 16-3
WS 16-1
TNU/FU
Section 18
ws 15-7
ws 15-12
WS 15-25
N17b
TKU/CU
ws 17-3
Section 15
NN11 WS 17-4
Section 17
TNU/FU
NN6
NN5 N9/10
NP23/24
Section 16
TRANSECT II
interbedded very thin ash layers
N17
N16
Section 2
Section 1
poorly exposed
N16 slidemass
reefal debris (Lepidocyclinids)
Section 9
interval estimated
N14/15
N(11)/12
Section 10
interval estimated
basement (porphyry)
N of Lewa
TRANSECT I

outcrops, regularly distributed along the 3 transects. From this material some 200 standard size specimens have been drilled in the laboratory. All specimens have been measured on a ScT cryogenic magnetometer for the detection of the intensity and direction of the characteristic remanence. Progressive demagnetization has been performed using standard demagnetization procedures with alternating magnetic fields (AF method), and with heating. The AF method has been applied in between 8 and 18 successive steps, with maximum peak values between 40 and 100 mT. Two specimens have been heated up in 16 successive steps with maximum temperatures above 600°C.

In order to prepare a synthetic seismic section, Transect II has also been sampled for petrophysical purposes. Due to the friable character of especially the sandier sediments, only a limited number of cores could be drilled in the laboratory to represent the 6 main lithologies for measurement of the acoustic properties (stratigraphic position indicated with WS numbers, Fig. 3). For a description of this modelling procedure the reader is referred to Van der Werff (1996, part 2). The results are compared to seismic profile PAC 109 (Fig. 2), a multichannel profile of Shell International Petroleum Maatschappij (The Hague) across Sumba Ridge, 70 km E of the stratigraphically most complete Transect II and revealing some striking similarities with the onshore geology.

Transect I combines sections oriented along a WSW-ENE line in the vicinity of the main road Waingapu-Lewa (Fig. 2B). These are all located W of fault zone F1, where the volcaniclastic supply was considerably less than further east. The paleomagnetic sites have been labelled ss.k–n; Fig. 2B). Transect II covers sections positioned in a more N-S line in between Waingapu and Tanarare, a village bordering the pre-Neogene Massu Mountains (Fig. 2A). The paleomagnetic sample sites have been labelled ss.f–i and ss.o-t. Transect III covers the easternmost sections recorded in the vicinity of the road Melolo-Kananggar (paleomagnetic sites ss.a–c; Fig 2B). The coastal cliff section of Leilunggi, has been added, but as it is located on the Indian Ocean side of the Massu Mountains it is correlated on the basis of biostratigraphic data only.

Middle to Late Miocene samples from Transects II and III often contain very poor planktonic foraminiferal associations due to carbonate dissolution, but calcareous nannofossils (biostratigraphic data kindly provided by B. Prins) give additional information. For the planktonic foraminiferal determination and biostratigraphic data, we largely follow the zonal scheme of Blow (1969), as emended by Bolli and Saunders (1985) and Chaisson and Leckie (1993), the latter based on studies of ODP sites on the Pacific Ontong Java Plateau. The ages of plankton datum planes used are mainly based on Berggren *et al.* (1995a).

Stratigraphy and sedimentation

This section gives an overview of the sedimentary data for each transect, followed by the biostratigraphic data which permitted the age assignments indicated in the columns (Fig. 3). The biozones are indicated to the right of the columns at those levels where they are for the first time certified in the sample record. The section ends with a discussion of sedimentary aspects and correlation of the sedimentary units.

Transect I (East Central Sumba)

General. The Neogene of Central Sumba is mainly developed in a pelagic chalky, or mixed chalky-marly facies. A total thickness of at least 450 m is estimated, with ages ranging from middle Miocene to early Pliocene (Fig. 3).

The basal Neogene is generally poorly exposed and varies laterally. West of Lewa (not in column), neritic marls rich in gastropods and the larger foaminifera ***Spiroclypeus*** and ***Cycloclypeus*** follow above massive Paleogene limestones. North of Lewa, approximately 20 m of massive, upward fining calcirudites and calcarenites onlap onto igneous basement rocks (Fig. 3, base of column). The skeletal limestones include reefal debris and the larger foraminifera ***Operculina,*** *Spiro-* ***clypeus, Miogypsina*** and ***Miogypsinoides.*** Towards their top these beds grade into mixed marly and calcarenitic intervals and upwards into predominantly marly chalks. Occasionally, thin, distal turbidites and/or ash layers occur. Such coarser interbeds may be almost obliterated due to intense burrowing. The strata are widely exposed in the hills along the road from Makaminggit eastwards, and are represented from base to top by Sections 10, 9, 1 and 2 (Figs 2B, 3).

The more than 100 m thick middle Miocene part (Sections 10, 9) is truncated by a 10 m thick calciruditic channel-fill, rich in reefal debris and Lepidocyclinids. Just above this level a 15 m thick slump occurs, which level marks the transition from dominantly calcarenites and chalks below, to the foraminiferal chalks (developed as marly chalk and chalky marl couplets of variable thickness) characterizing the younger deposits. Some beds include pumice fragments and occasionally alternate with strongly burrowed ash layers.

Section 24 is an isolated cliff outcrop along the Kapunduk River near Rambangaru (Figs 2B, 3). Here the Mio-Pliocene boundary can be detected near the top of a 120 m sequence of well exposed homogeneous foraminiferal chalk-marl couplets suggesting Milankovitch rhythms. Intercalated distal turbidites are mainly confined to the lowermost Pliocene (100-l 10 m).

Biostratigraphic data. A well preserved assemblage from the basal strata includes abundant ***Globorotalia*** *mayeri* and ***Globoquadrina altispira, var.*** *conica*, which together with ***G. obesa, G. praemenardii*** and G. ***fohsi lobata*** indicate Zone N(11)/12. The base of Section 10 thus was deposited around 12.7712 Ma during the Serravallian. Its top reaches into Zone N14/15 (11.7-l 1 Ma), as indicated by the presence of ***G. challengeri*** and ***G. menardii*** forms 1 and 2 of Tjalsma (1971). Also the chalks underlying the channel at the base of Section 9 still indicate a middle Miocene age ***(G.*** *mayeri*, ***G. praemenardii),*** whereas the chalk immediately above it already includes an assemblage indicating Zone N 16 (Tortonian; abundant ***G. menardii; dextral G. acostaensis;*** *G*. ***merotumida).*** This result indicates that the channel level represents a hiatus.

Both Section 1, and the base of Section 2 yield microfaunas characterized by abundant ***Orhulina, Globoquadrina altispira, Sphaeroidinellopsis*** *sp*., and

commonly sinistrally coiled G. ***menardii.*** Together with ***Neoglohoquadrina acostaensis*** a late Miocene age can be concluded (Zone N 16). Approximately 70 m above the base of the section ***Globorotalia*** *cibaoensis* makes its appearance, which indicates a position close to Zone N 17. This zonal boundary is probably 25 m higher, where ***G. plesiotumida*** enters the section.

Section 24 (Rambangaru) comprises well preserved foraminiferal faunas that can be attributed to Zone N 17 ***(G.*** *cibaoensis*, ***G. juanai; G. plesiotumida;*** common N. *humerosa* and ***G. menardii).*** The first occurrence (FO) of *Pullenia primalis* (FAD at 6.4 Ma, Berggren ***et al.*** 1995a) at the level of 63.5 m indicates the transition to Zone N 17b (Chaisson and Leckie 1993). At 97.5 m ***Globorotalia*** *tumida* makes its appearance, so that this upper part of the section can be correlated with Zone P11 of Berggren *et* ***al.*** (1995a; FAD at 5.6 Ma) and just reaches into the early Pliocene.

Benthic foraminifera are more common in Section 10 than in the younger Sections 1 and 2. All assemblages, however, reflect open marine environments indicated by the high to very high amounts of planktonic foraminifera. Deep water benthic species, such as e.g. *Melonis* ***barlaeanum*** have not been observed in the older to middle Miocene assemblages. With the base of the section consisting of neritic limestones, an overall M. Miocene deepening evidently took place; the benthic foraminifera suggest deepening to > 1000 m. The assemblages of Section 1 seem to have been affected by some partial dissolution. Partial fauna1 dissolution (lysocline influence) also affected assemblages of Section 11 (Fig. 3B: south coast) where some samples almost exclusively consist of *Sphaeroidinella* sp. and occasional ***G. acostaensis*** and ***G. menardii,*** specimens, indicating a late Miocene age.

The youngest sediment sampled in central Sumba is a foraminiferal chalk exposed south of Lewa. The well preserved assemblage belongs to Zone N 19/20, as indicated by the co-occurrence of ***Globorotalia*** *crassaformis* and dextrally coiled *Pulleniatina* ***primalis.*** Because the sinistral to dextral coiling change of the latter species takes part at 3.95 Ma (Berggren et ***al.*** 1995b) it is concluded that bathyal conditions continued in Sumba for most of the Early Pliocene.

Transect ***II (Waingapu-Tanarare)***

General. Transect II differs from the succession along Transect I by the relative importance of volcaniclastic turbidites. The stratigraphically most complete record occurs between Tanarare and Hiliwuku (Figs 2A, B). This 400 m thick succession extends from an angular unconformity, separating the underlying and faulted Paleogene limestones of the Massu Mountains, to the early Pliocene (sections 15–18, Fig. 3). Sections 12 and 14 (Figs 2B, 3), located further north in the Waingapu area. give additional information about the latest Miocene-early Pliocene. Based on main trends in the relative proportion and average grain size of the volcaniclastics, an informal division into five sequences is made (units A-E, Fig. 3). The turbidites represent mixtures of volcanogenic, bioclastic and pelagic material that are barely affected by diagenetic processes. The lithological constituents are varying percentages of minerals such as augite, quartz, plagioclase, amphibole and hematite mixed with pumice, glass shards and bioclastics. The grains are cemented by lime mud and are either matrix or grain supported. The intercated grey and beige chalk-like beds constitute both hemipelagic nannofossil oozes and volcanigenic muds. As discussed by Fortuin et ***al.*** (1994a) paleocurrents measured along Transect II are mainly oriented to the NNE, but directions to NNW were also observed.

Unit A. In section 16 (3 km west of Tanarara; 10°00′22 S; 120’16’44 E) an angular unconformity separates Paleogene ***Nummulites*** limestones of the Paumbapa Formation from a 3 m basal conglomerate, overlain by 12 m of homogeneous marls. The transgression conglomerate is composed of well-rounded clasts derived from the underlying unit. An erosional surface separates this unit from the first volcaniclastic turbidites and pumiceous debris flow deposits. Volcanic glass shards, however, already occur in the marl interval.

Unit ***B.*** This unit comprises approximately 25 m of thick-bedded turbidites, poorly exposed in the cliffs southwest of Tanarare (Section 17, not sampled). Because these beds are truncated by Unit C these deposits are absent 3 km west of Tanarare, where unit A and overlying strata were studied (section 16).

Unit ***C.*** This unit consists of volcaniclastic mass flow deposits, turbidites, and interbedded hemipelagic muds showing an overall fining-thinning up trend. On a smaller scale various fining-/thinning-up and upward coarsening-/thickening sequences can be distinguished. In the extremely sand rich lower part of the unit, amalgamation of the turbidites is common (turbidite facies types A-B of Shanmugan and Moiola 1991; Mutti 1992). Several intercalated megabeds, consisting of a chaotic mixture of boulders and slumped strata (Facies F of the latter authors), grade towards their top into normal turbidites. Near Tanarare, such a slump, up to 30 m thick, can be seen to develop laterally by stepwise cutting into the underlying strata. Some kilometres further to the north this bed passes into a thick turbidite with a muddy-gravelly basis. Bouma $T_{b\ c}$ turbidites are common in the finer grained intervals.

The turbidites in the upper part of Unit C are often developed as Bouma $T_{c\ d}$ sequences, although thick-bedded, horizontally laminated turbidites are still common. A general decrease in sand/marl ratio from 2: 1-l : 1 is observed.

Unit D. The transition to Unit D is characterized by the reappearance of very thick, clast-supported debris flow deposits and turbidites, which grade at their top into sandy, laminated intervals (Section 15, 6 km south of Hiliwuku; 9°55′26 S; 120°19′34 E). The upper part shows a fining-up tendency (Figs 4A; 8), due to the gradual disappearance of volcaniclastic turbidites. In the hemipelagic interbeds planktonic foraminifera gradually make their reappearance.

The very thick sandy and gravelly mass flow deposits are often associated with thickening and coarsening-up sequences. In the pumiceous gravels both normal and inverse grading can be observed (Fig. 4B). Frequently occurring mudballs indicate considerable erosion of the sea floor. In contrast, the relatively fine grained intervals are rich in distal, thin-thick bedded $T_{b\ d}$ and $T_{c\ d}$ turbidites, showing well developed climbing ripple sets (Fig. 4C, D) and convolute lamination. Also these turbidite soles frequently reveal scouring of the underlying muds, whereas the upper laminated intervals are often intimately mixed with the overlying

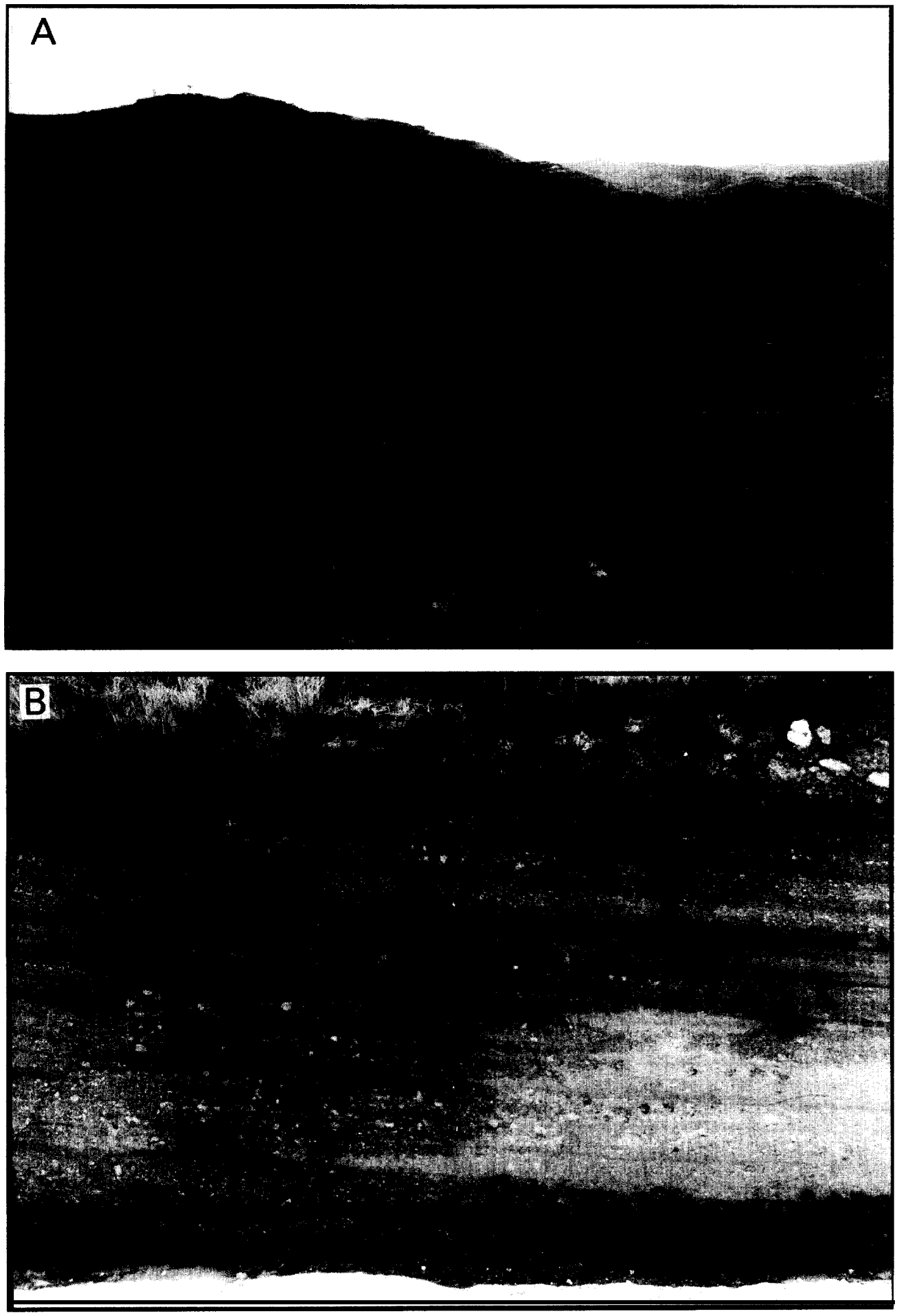

Figure 4A and B.

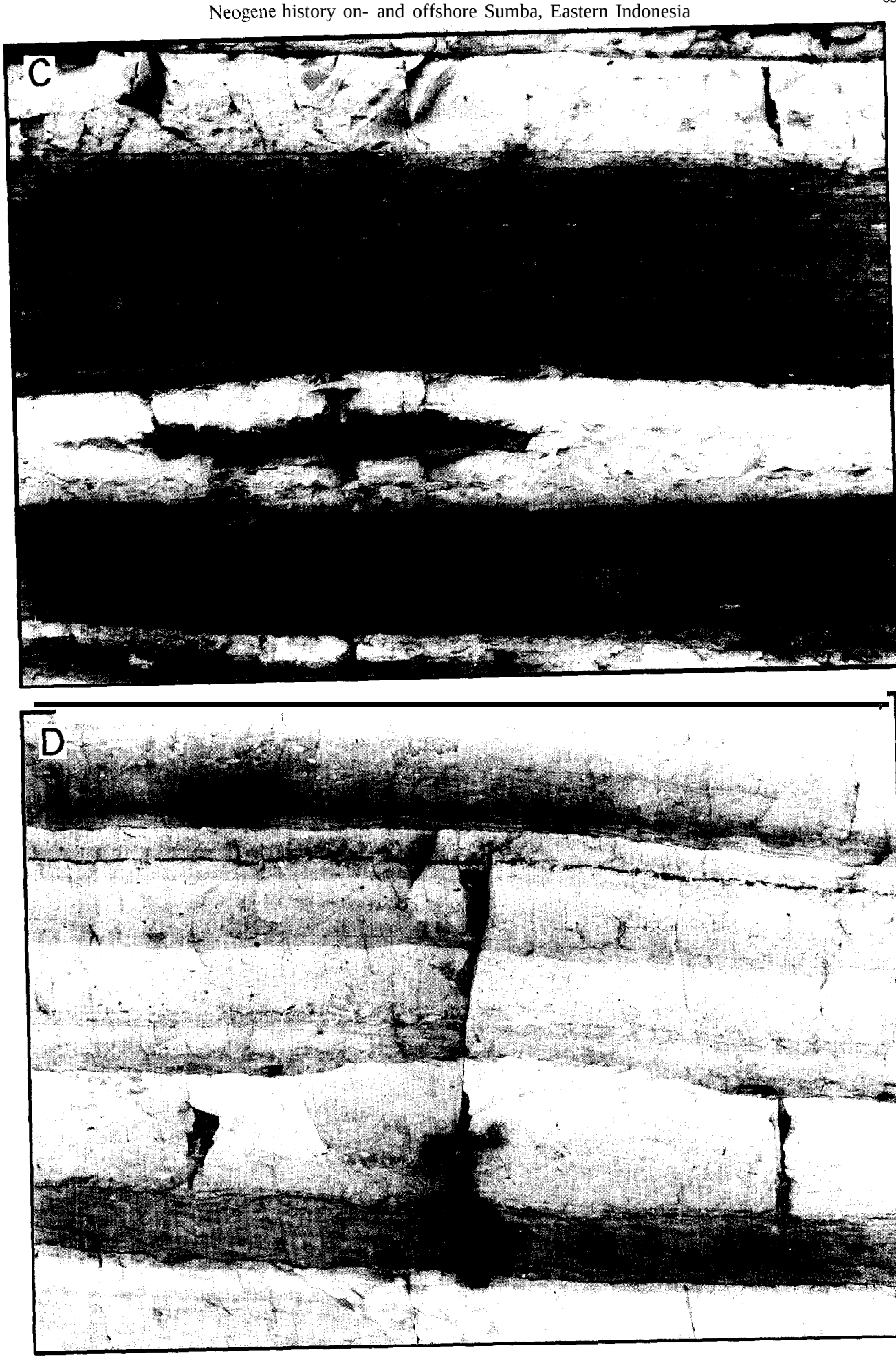

Figure 4C and D.

hemipelagic muds, due to intense bioturbation (Fig. 4D).

Unit E. This unit characterized by chalk-marly chalk couplets, starts above the last very thick turbidite bed, just below the road level of section 18 (located 2.5 km south of Hiliwuku, 9 54'03 S; 120 19'3 1 E; Fig. 8). Part of this unit has been sampled for magnetostratigraphic correlation of the Mio-Pliocene boundary.

Further north, the Kambaniru River outcrops (section 12; Figs 2B, 3) provide a lateral equivalent of Unit D. Two up to 10 m thick volcaniclastic megaturbidites occur, which beds are considered intermediate between matrix supported gravels and slumps (Fortuin *et al.* 1992, Fig. 5). Unit E is represented by section 14 (Figs 2B, 3), which exposes 50 m dominantly marly and chalky strata. Distal turbidites, intercalated near the base of the section, show N-oriented current ripples. A particular outcrop within this unit (Roep and Fortuin 1996) exposes a submarine slide scar, filled with slide blocks and megarippled *Glohigerina* sands of possibly contourite origin.

Biostratigraphic data. Nannofossil assemblages from the base of Unit A indicate reworking of sediments of Cretaceous and late Oligocene age. The latter age (upper NP 23/24) is also given by a chalk sample at the unconformity, demonstrating that carbonate platform deposition continued at least until the late Oligocene. Co-occurrence of the calcareous nannofossils *Sphenolithus hetermorphus* and *Eudiscoaster signus* in the lower part of Unit A indicate Zone NN5, proves that deposition was re-established during the Middle Miocene. The nannofossils in the higher part of Unit A can be assigned to Zone NN6, by the association of abundant *Reticulofenestra floridana/abisecta* and *Eudiscoaster bollii,* with absence of *S. heteromorphus*. These results indicate a late Langhian to Serravallian age (max. 15.6-l 1.9 Ma) for this condensed unit. Planktonic foraminiferal assemblages confirm this age: chalk intercalated in the basal conglomerate includes *Globorotalia peripheroacuta, G. sp* cf. *hirnageae,* plus *G. mayeri/siakensis* and *Globigerinoides diminutus. G. peripherorondu* (LAD at 14.6 Ma) has also been observed near the base of this unit. The combined data indicate that open marine sedimentation started during biozones M6-7 (= N9/10), i.e. from approximately 15 Ma onwards.

Benthic foraminifera present in a sample **just** above the unconformity, still indicate outer-neritic depths, as can be concluded from the low plankton percentage (approximately 10%, with only small Globigerinids), absence of typical deeper water forms so common higher up, versus abundance of shallow outer-neritic species such as *Cibicides refulgens*, *Rotalia sp.*, *Elphidium crispum*, *Planorbulinella mediterranensis* and *Amphistegina lessonii.* Already within the conglomeratic interval a change to a bathyal, pelagic environment can be concluded from the change to scarce benthic foraminifera and abundant plankton. Continued deepening is concluded from the first indications for strong fauna1 dissolution towards the top of Unit A, where occasionally occurring forms such as thick walled *Globoquudrina altispira,* **var.** *conica* and rare *G. mayeri* are the only fauna1 remains due to dissolution near or below the carbonate compensation depth (CCD; Fortuin *et al.* 1994a).

Biostratigraphic subdivision of the major part of Transect II is difficult, due to the effects of dissolution. Only the relics of thick walled species like *Sphaeroidinellopsis* and/or small Globigerinids are present in part of the samples. Less dissolution-affected foraminiferal assemblages gradually reappear in the upper part of Unit D. Abundant reworked foraminifera, however, occur in the laminated intervals of the turbidites, which often also include benthic species of shallow marine origin. *Globorotulia menardii* (sin.) is common in a reworked assemblage in the lower half of Unit C, suggesting a late Miocene age. Nannofossil assemblages from the middle and upper part of Unit C indicate a middle-late Tortonian age (NN 11) by abundant *Eudiscoaster quinqueramus* and absence of *Amaurolithus* sp. The erosional unconformity separating Unit A from (B)C units therefore most probably is a lateral equivalent of the erosional gap observed in Transect I and interpreted as a sequence boundary separating middle and late Miocene sedimentation.

In Unit D, the first better preserved planktonic assemblages start from the level of approximately 260 m up. The genus *Sphaeroidinellopsis* is abundantly represented. A latest Miocene (Messinian) age (N17b) is indicated by the presence of *Pulleniatina primalis* and dextrally coiled *Neogloboquadrina acostaensis*, and higher upwards also *Globorotalia conglobatus.* The transition towards Unit E takes place close to the Mio-Pliocene boundary. as indicated by the first occurrence (FO) of *G. tumida.* and discussed in the section on magnetostratigraphy.

In the Waingapu area, Section 12 is correlated with

Fig. 4. Photographs showing various aspects of the volcaniclastic turbidites in Transect II. In B, C and D hammer for scale.

A. Bedding pattern in the middle-upper part of Unit D. Note the various smaller upward thickening sequences in the lower half of the valley (approximately 80 m deep) and the overall thinning- and fining-up towards the top. The bedding rhythms can be traced laterally for kilometres. A minor fault to the right of the picture is indicated with a broken line.

B. Partial exposure of a very thick, matrix-supported and pumice-rich gravel bed (Unit D), showing both normal and inverse multiple grading.

C. More distal turbidite variety in unit D, showing a well developed, but crudely laminated T_B interval, a feature common in pyroclastic turbidites due to rapidly fluctuating density contrasts. Also the climbing ripple intervals are often well developed. Unusual is the laterally restricted bed near the hammer, probably due to partial homogenization of this sandy bed by strong bioturbation.

D. The most distal Tb-d turbidites of unit D still show moderate scouring at the base, followed by crude, but well developed horizontal lamination and convoluted climbing ripple sets. The top of the turbidites tend to be strongly burrowed.

nannofossil Zone NN1 lb (Messinian) by the abundance of *Eudiscoaster quinqueramus* and presence of *Amaurolithus*. The planktonic foraminiferal assemblages are still poorly preserved. Section 14, can be attributed to the early Pliocene (Zone NN13/15).

Transect III (Kanaggar-Melolo)

Despite its thickness of 600 m, Transect III is stratigraphically less complete because the latest Mio- and Pliocene appear to be missing. It is characterized by the presence of large sediment slides, exposed over at least 10 km' in the area between Kananggar and Maumaru (Fortuin *et al.* 1992; Fig. 2B, 3). Much of Transect III can be studied in the surroundings of Kananggar (10°5'14 S; 120°2 1'24 E; Sections 4 A-D). Because previous authors did not indicate a type locality for the Kananggar Formation, we propose Section 4 as the formal stratotype. Unfortunately, the contact with the underlying units is not exposed in this area.

Four units are distinguished, here numbered 1–4 as they are different from the A-E units of Transect II:

Unit 1. The basal unconformity has not been observed near Kananggar. The first exposed 85 m has a sand/mud ratio of 1:4 and is dominated by grey mottled tuffaceous mudstones, alternating with dark thin volcaniclastic T_b turbidites and fine-grained glassy interbeds (Section 4A; exposed from Kananggar uphill along the road to Leilunggi).

Unit 2. Between 85 and 210 m, an overall thickening and coarsening-up trend is evident. The unit is characterized by the common presence of very thick volcaniclastic turbidites, followed upward by extremely thick pumiceous debris flow deposits. The latter deposits are slightly cemented and crudely amalgamated. The thickest bed (36 m) includes boulder-sized fragments of pumice, basalt, limestone and marl intra-clasts. Various stacks of smaller thinning up and thickening up cycles can be distinguished. Due to the rapid transitions from amalgamated massive sand and gravel bodies to individual beds, the strata1 pattern is rather irregular. Fortuin *et al.* (1994a) figured and interpreted this unit as part of a channel complex that truncated the underlying beds at a low angle.

Unit 3. This interval consists of two sediment slides respectively up to 130 m and 20 m thick and both ending in dominant mudstones (Sections 4B, C; figured in Fortuin *et al.* 1992). A special feature is the presence of a 70 cm thick graded foraminiferal chalk bed, located just above the largest slide. Although thin foraminiferal turbidites occasionally occur in these microfauna poor successions, this is the only bed observed of that size.

Unit 4. The upper 50 m of the Kananggar succession is characterized by a sand/mud ratio of 1: 1 and is rich in volcanic glass shards. Very thick turbidites are restricted to the basal part and are characterized by well developed T_b intervals with frequent convolute bedding (N-directed paleocurrents; Section 4C). The base of Section 6 (Maumaru, 100'00'27 S; 120°29'57 E) starts above a major slide which probably correlates with the second slide of Section 4. This section exposes more than 150 m of thin to thick-bedded turbidites and interbedded grey hemipelagic muds arranged in about 10 coarsening and thickening-up cycles. Towards the top the sand/marl ratio has dropped below 1: 10.

Biostratigraphic data. Nearly 50 samples were studied from the pelagic intervals of this transect. Most proved to be barren, or nearly so. Only ghosts, or fragments of foraminifera occur, with occasionally thick walled species like *Sphaeroidinellopsis*, or minute Globigerinids and other fragments. For an age assignment of the older part of the transect, we rely on age dating by C. Miiller (in Burollet and Salle 1982), who concluded a Tortonian age.

Nannofossils from Section 6 indicate that this part can be correlated with Zone NN1 la (younger Tortonian), due to the abundance of *Discoaster quinqueramus* (with *Sphenolithus abies, D. pentaradiatus* and small *Reticulofenestra sp.)*. Due to the occurrence of (poorly preserved) *Amaurolithus sp.,* at the top, it is likely that the uppermost meters straddle the Tortonian-Messinian boundary. The first foraminiferal assemblage was also sampled from this level and agrees well with the latter data (N17; lower Messinian by presence of *Globorotalia plesiotumida* with dextral *Neogloboquadrina acostaensis* and absence of *P. primalis).*

Some well preserved foraminiferal assemblages were observed in mudballs in volcaniclastic turbidites. This fact, plus the presence of several foraminiferal turbidites, underscores the importance of fauna1 dissolution after deposition. A mudball from the lower part of Unit 2 clearly indicates the reworking of middle Miocene pelagic muds, as shown by the association of *Globorotalia mayeri/siakensis* and the *G. fohsi lobata* and *G. fohsi robusta*.

Also the samples from Section 5, located near the south coast, proved to be almost barren due to fauna1 dissolution. One better preserved assemblage must be related to reworking, as is indicated by the mixing of shallow marine fauna (coral debris, *Lepidocyclina)* and Middle Miocene taxa such as G. *kugleri.* Because the youngest nannofossils from this sample also indicate this age (NN 5 by presence of *Sphenolithus hetermorphus, abundant S. abies, S. moriformis*, *Reticulofenestra pseudoumbilicus* and *R. antarctica,* no younger taxa), it is concluded that Section 5 represents the erosion relic of an older part of the volcaniclastic sequence than found in Transects II and III.

Early Pliocene chalks were sampled from minor exposures along the north coastal area, east of Melolo. This suggests that younger strata originally have been deposited, but largely were eroded after the emergence of Sumba.

Correlations and depositional patterns

The composition of the volcaniclastics, so abundant in transects II and III, reflects island arc volcanism (Fortuin *et al.* 1994a). This was also concluded from the calcalkaline affinity and trace-element signatures of the Paleogene andesitic lavas of the Jawila Formation in west-central Sumba (Wensink and Van Bergen 1995).

Transects I and II can be correlated on the base of an erosional hiatus occurring at the boundary between the Middle and Upper Miocene sediments. This sequence boundary followed after a period of considerable deepening of Sumba during which east Sumba subsided more strongly and where CCD depths were reached prior to the Tortonian. The fast upward change within unit A of Transect II of outer neritic to abyssal

environments is interpreted as a combination of rapid subsidence and very little sedimentation. The Tortonian turbidite sequence of unit C of Transect II can be correlated with most of Transect III (units 24). The role of unit B is doubtful, because age data are lacking.

The general picture that arises from field observations on the turbidite sequences is one of stacked patterns of shifting fan lobes, which partly truncated and partly onlap older sequences. Sediment accumulation rates thus will have varied considerably over short distances. An exception to this general lobe pattern is Kananggar unit 2, Transect III, which displays the complex strata1 pattern resulting from stacked channels. The unit can be traced in the field towards the relatively coarse clastic mass flow rich base of unit C, Transect II. The Kananggar channel complex and major slump intervals suggests that Transect III was located on a suprafan lobe very close to a main channel system. The reduced thickness and overall finer grained character of Unit C of Transect II (with the presence of abundant $T_{c\ d}$ turbidites), is more suggestive for a region of significant sediment bypass such as a levee or the outer side of a suprafan lobe (Walker 1992). The Kananggar megaslides (Unit 3, Transect III) probably reflect instability and tectonic activity during fan growth. Walker (1992) pointed out that such mass transport complexes can be related to sea level changes, but regarding the interpreted abyssal environments, their proximity to a convergent margin and the likely presence of submarine slopes surrounding the volcanic source(s), tectonics will have played a major role. The resulting morphologic changes may have caused a shift in lobe deposition, after which the outerfan sediments of Unit 4 (Transect III) were deposited.

The lateral continuity of the thick bedded debris flow deposits and turbidites of Unit D (Transect II) and the absence of channelling are indicative for suprafan lobe deposition downslope of a main channel system (Mutti and Normark 1987). These deposits may have filled in the depression formed above Unit C (Transect II).

As most volcaniclastic sequences occurring north of the Massu block are of late Miocene age, the presence further south of the lithologically similar middle Miocene section 5 is an important fact, as it proves the existence of a related middle Miocene generation of volcaniclastic turbidites. Considering the generally northward oriented paleocurrents and presence of middle Miocene mud-lumps in late Miocene turbidites it is suggested that all east Sumba Kananggar deposits together represent different parts of an emerged Miocene northward prograding deepsea fan, in which the older parts are better developed towards the south.

Concluding, the overall sedimentation pattern reflects major volcaniclastic supply during the Serravallian (Section 5, Fig. 3), and early-middle Tortonian times, a waning supply during the later Tortonian and a renewed supply during the Messinian. The volcanic origin of most of the detritus suggests that variations in volcanic activity governed the growth of the fan deposits. In addition to episodic growth of the volcanic edifice and concomitant supply of volcaniclastics, eustatic sea level changes will also, to a certain extent, have left their imprint on the sedimentary record. This could be the case in Transect I, where the erosional unconformity at the base of the Tortonian seems coeval with the sequence boundary separating the TB2/TB3 supercycles of the Haq *et al.* (1988) cycle chart, which boundary is said to be well developed in the Flores Sea (Bartek *et al.* 1991).

Paleomagnetism

Paleomagnetic results from the study of the Kananggar Formation have been documented to constrain the final stage of the drift of the Sumba fragment since late Miocene-early Pliocene time. The rock magnetic properties have been determined to get insight in the carriers of the magnetic remanence, and the grain size of these minerals. In addition, the results are given of a detailed paleomagnetic study for the possible detection of the Mio-Pliocene transition using geomagnetic polarity reversals, in order to test the potential use of late Neogene Sumba sections for future stratigraphic work. Although the results are encouraging and need to be communicated, they are preliminary.

Characteristic remanence directions

The initial remanence intensities of the sediments of the Kananggar Formation show large variations between 1 and 300 mA/m (Table 1). During progressive demagnetization the behaviour of the remanence vector indicates that most samples have a small viscous component of magnetization. This disappears either after AF treatment between 5 and 10 mT peak value, or after heating at 100–150°C (Fig. 5). During progressive demagnetization, the intensities decrease rather rapidly: after AF treatment in fields of 20 mT maximum peak value, often less than 50% of the initial remanence is left; after heating at 560°C, a maximum of 5% of the initial remanence is left, indicating that magnetite probably is the main carrier of remanence (Fig. 5).

Table 1. Rock magnetic properties of sediments from the Kananggar Formation, Sumba, Indonesia. J_0 is the initial remanence intensity in mA/m; IRM (2.5 T) is the isothermal remanence in mA/m after application of a maximum direct field of 2.5 Tesla; Hcr(mTesla) is the remanent coercivity force in mTesla; x-0 is the low-field susceptibility in SI-units

Specimen	Jo	IRM(2.5T)	Hcr(T)	x-o
SS.A3	16.5	587.6	0.0441	4.50E-04
SS.B2A	4.1	250.7	0.0610	2.40E-04
SS.C4A	4.8	261.0	0.0538	2.60E-04
SS.D1A	18.9	2629.7	0.0275	1.95E-03
SS.D2A	33.9	2133.1	0.0286	1.70E-03
SS.E4A	33.7	3193.9	0.0244	2.73E-03
SS.F3	3.5	128.7	0.0420	1.80E-04
SS.G1	2.0	182.6	0.0630	2.10E-04
SS.H4A1	3.1	272.6	0.0840	2.20E-04
SS.I11	4.7	607.8	0.03 15	6.1 OE-04
SS.K3	40.6	1096.6	0.0270	9.90E-04
SS.L41	17.1	787.4	0.0280	7.50E-04
SS.M3	8.4	205.3	0.0638	1.30E-04
SS.N4	3.4	151.7	0.0385	2.00E-04
SS.P3A	1.3	114.2	0.0747	1.30E-04
SS.Q4A	3.0	144.0	0.0454	1.70E-04
SS.R2A	24.6	7930.6	0.0442	5.39E-03
SS.S2A	52.7	2424.7	0.0694	1.76E-03
SS.S4A	2.1	184.6	0.0769	2.20E-04
SS.T4	236.9	6472. 1	0.0377	6.63E-03
SS.T5	172. 1	63 14.7	0.0374	6.45E-03

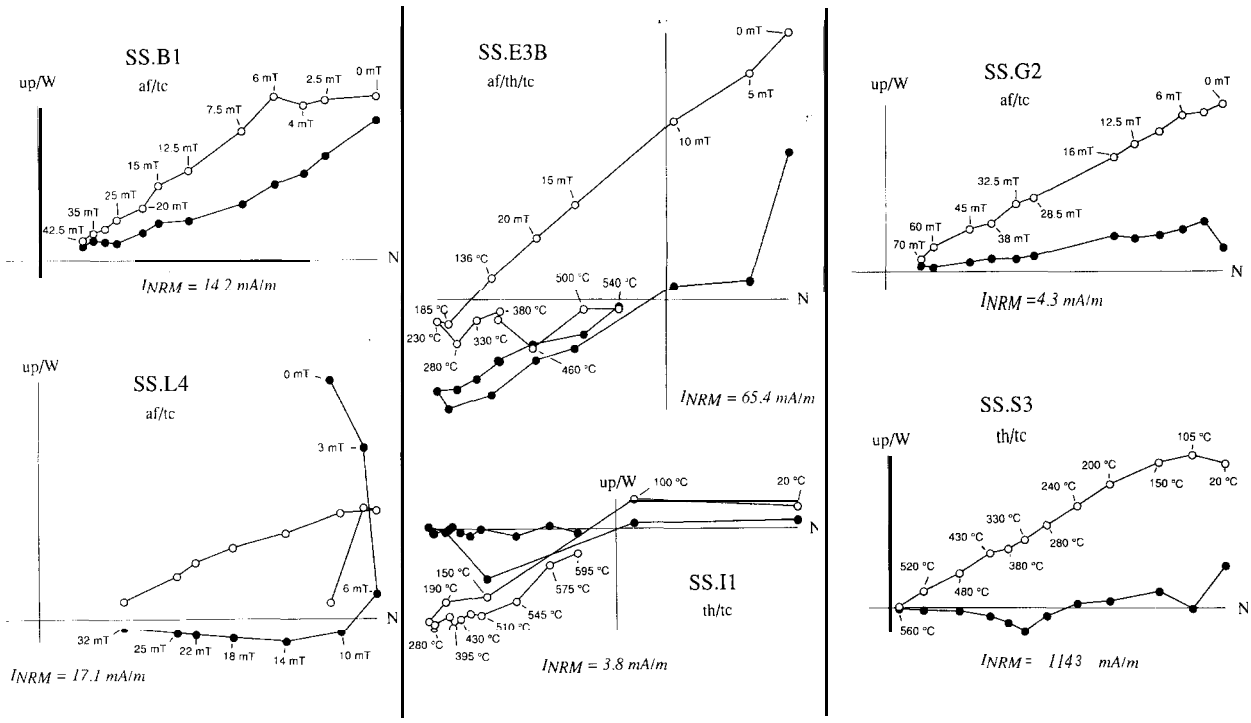

Fig. 5. Diagrams showing the progressive demagnetization of specimens from the Kananggar Formation: by alternating magnetic fields (SS.B1, SS.G2, SS.L4), by heating (SS. I1, SS.S3), and by alternating magnetic fields and subsequent heating (SS.E3B). The plotted points represent successive positions of the resultant remanence vector in orthogonal projection. Closed (open) circles denote the projections on a horizontal (vertical) plane. Peak field strengths are given in mT (1 mT = 10 Oerstedt); temperatures are given in Celsius. I_{NRM} is the initial intensity of the natural remanent magnetisation (NRM) in mA/m.

In general, specimens with a normal polarity (negative inclinations and northerly declinations) do not show a secondary component of remanence. After removal of the viscous component, the characteristic component of remanence (ChRM) was isolated in specimens SS.B1, SS.G2, and SS.L4, but specimens SS.E3B and SS.I1 show a different behaviour (Fig. 5). Specimen SS.E3B has been treated with AF demagnetization to 20 mT peak field and subsequently heated to 540 C, specimen SS.I1 was heated to 595°C. Both specimens have a large component of secondary magnetization, that disappears after heating at 240°C. The remaining ChRM direction of these specimens has a reversed polarity (positive inclination and approximate southerly declination). The secondary component of magnetization is directed approximately antiparallel to the ChRM direction. This component was acquired during a time of normal magnetic polarity. Because the ChRM directions found in the Kananggar sediments are not significantly different from the direction of the earth's present day magnetic field, the time of the remagnetization cannot be given. Specimen SS.S3 is a good example of progressive heating with a ChRM direction of normal polarity (Fig. 5). Progressive heating was often successful (Fig. 5: SS.I1) when the specimens have a low initial remanence intensity and a reversed polarity.

Rock magnetic properties

From one specimen of each site the rock magnetic parameters were determined. For a number of specimens, acquisition curves of the isothermal remanent magnetization (IRM) were made, using a PM 4 pulse magnetizer (maximum peak direct field of 2.5 Tesla). These specimens are saturated after a direct field of 0.3 to up to 0.5 Tesla (Fig. 6). IRM (2.5 Tesla) data are listed in Table 1. With values ranging between 0.1 and 7.9 A/m, it is clear that there are large differences in concentration and/or nature of the magnetic minerals.

Normalized remanent hysteresis curves (Fig. 6: upper row) and acquisition curves (Fig. 6: lower row), show that some specimens (SS.L41) more rapidly increase in remanence intensity with increased applied field than others (SS.S4A).

For at least one specimen per site, the remanent coercive force (H_{cr})has been determined, i.e. the strength needed to reduce the IRM (2.5 Tesla) to zero. The results (Table 1) show large differences in H_{cr} values ranging from 0.024 to 0.084 T. H_{cr} values of approximately 0.03 T in combination with very small grain sizes of 5 μm or less are indicative for (titano-)magnetite as the main carrier of remanence (Hartstra 1982). An increase in grainsize causes the H_{cr} value to decrease rapidly. A rapid increase of IRM at low applied direct fields (up to 0.2 T) points to the presence of a low coercivity mineral, e.g. magnetite (Fig. 6: SS.L41, SS.D2A). Several specimens revealed rather high H_{cr} values (Table 1), pointing to the presence of hematite, usually corresponding to a rather slow increase in IRM intensity (Fig. 6: SS.S4A, SS.S2A). Indeed, from progressive heating, we concluded that in some specimens hematite must contribute to the remanence (Fig. 5: SS.I1).

Similar to the IRM (2.5 Tesla), the initial susceptibilities (x_0) show considerable variation (Table 1). From a large number of specimens both the (x_0) and the ($x_{0.025T}$) — the susceptibility after AF treatment in 0.025 T peak value — have been determined, illustrating a consistent

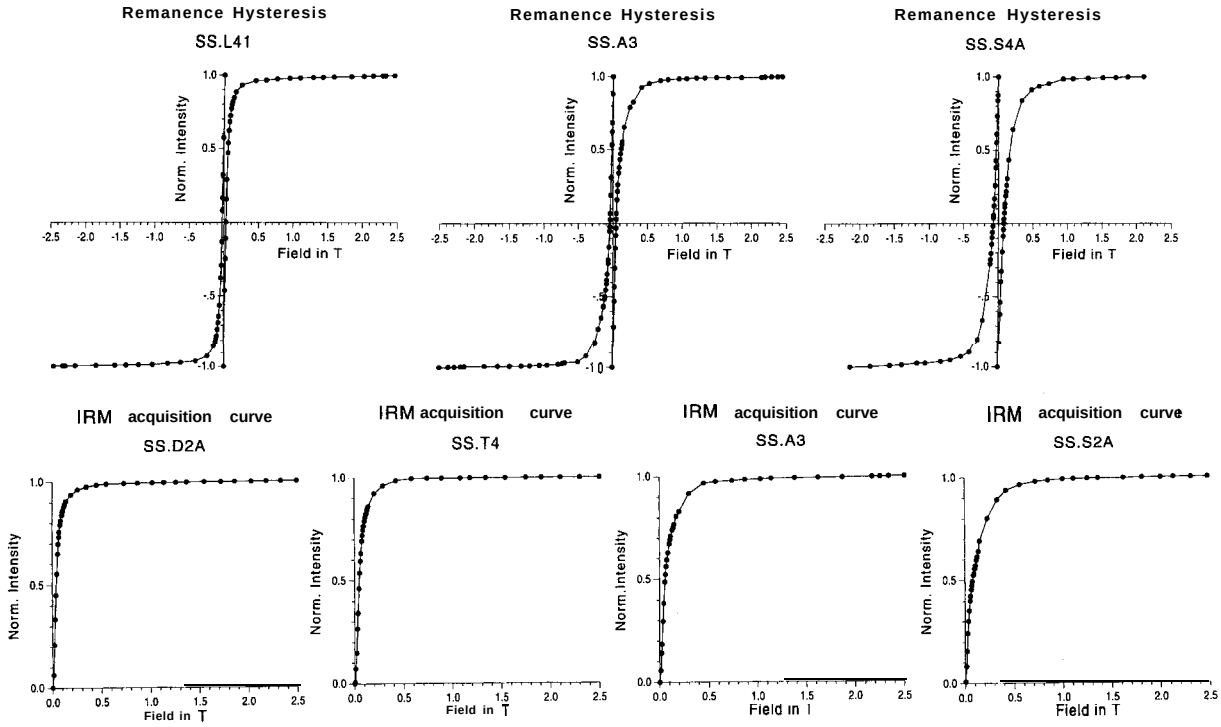

Fig. 6. Remanence hysteresis curves (above) and isothermal remanent magnetisation (IRM) acquistion curves (below) of specimens from the Kananggar Formation. The left curves in the upper row show the decrease to zero and the subsequent increase of remanence intensity in an opposite direct field of increasing strength up to 2.5 Tesla after application of a direct field of 2.5 Tesla. The starting point in the curves to the right is the IRM obtained after application of an opposite direct field with maximum strength of 2.5 Tesla. From these curves the, H_{cr} (remanent coercive force) is indicative for the carriers of remanence: rapid increase in remanence in intensity points to the prevalent presence of magnetite (SS.L41) and (SS.D2A); a more gradual increase in intensity points to the presence of hematite as the (partial) carrier of the remanence (SS.S4A, SS.S2A).

Table 2. Paleomagnetic data of the Middle Miocene-Early Pliocene sediments from central and east Sumba, Indonesia. N is the number of specimens included in the final analysis; D and I are the declination and inclination in degrees of the characteristic remanence direction; k is the precision parameter; a95 is the semi-angle of the cone of 95% confidence in degrees; N/R in the Polarity row means that specimens with both Normal and Reversed polarity occur; SS (bold) gives data of combined sites; ') sites SS.E and SS.O 1 + 2 only; ") site SS.E with E-l and E-2 and site SS.O with O-1 and O-2

Site	N	D	I	k	a95	Polarity	N*	X-25 mT s.d.	N**	x-38OC
SS.A	12	345.6	– 25.3	124	3.9 N	–				
SS.B	7	4.1	– 19.9	1149	1.8 N					
ss.c	7	1.3	19.3	105	5.9 N					
SS.D-I	6	0.2	– 4.7	266	4.1 N		–			
SS.D-2	8	354.5	11.7	269	3.4 N					
SS.E-I	6	346.8	– 29.5	52	9.4 N					
SS.E-2	5	162.9	12.8	93	8.0 R					
SS.E-1 + 2	11	344.9	21.9	38	7.5 N/R			3		30.38
SS.F	8	359.4	– 26.6	70	6.7 N	6	1.50	0.59		
SS.G	8	355.9	– 24.5	91	5.8 N	7	1.91	0.98	1	7.18
SS.H	8	346.0	31.0	24	11.6	N/R	5	2.38	2.08	1 3.58
SS.I	8	178.7	24.6	20	12.8	N/R	3	3.30	1.07	2 4.80
SS.K	8	352.1	21.4	162	4.4 N	4	4.95	0.82	1	18.24
SS.L	6	0.8	27.0	89	7.1 N/R	4	3.78	0.82	1	14.80
SS.M	9	1.0	– 26.3	99	5.2 N	5	2.97	1.98	1	4.98
SS.N	10	349.1	30.7	93	5.0 N	7	5.61	3.30	2	13.73
ss.o-I	6	350.6	28.2	36	11.3	N				
ss.o-2	5	190.7	20.9	59	10.0	R				
ss.o-I + 2	10	358.4	– 25.4	27	9.4 N/R	8	1.86	1.38	1	– 0.24
SS.P	7	174.9	26.0	36	10.2	R/N	5	4.10	2.96	1 12.24
SS.Q	8	163.2	27.9	37	9.3 R/N	7	2.90	1.84	2	5.37
SS.R	4	3.5	17.0	52	12.8	N	1	1.76		1 19.99
ss.s-1	9	356.5	– 22.7	76	5.9 N	7	4.29	1.29	1	20.59
ss.s-2	7	356.6	– 16.1	278	3.6 N	6	2.72	1.41	2	10.84
SS.T	9	0.5	19.3	41	8.1 N/R	10	5.52	1.13	2	25.96
SS′	21'	355.8	– 22.8	88.2	3.4 N	15"'	3.30	1.36	15"'	12.83
SS″	23"	355.6	– 22.8	73.1	3.6 N					

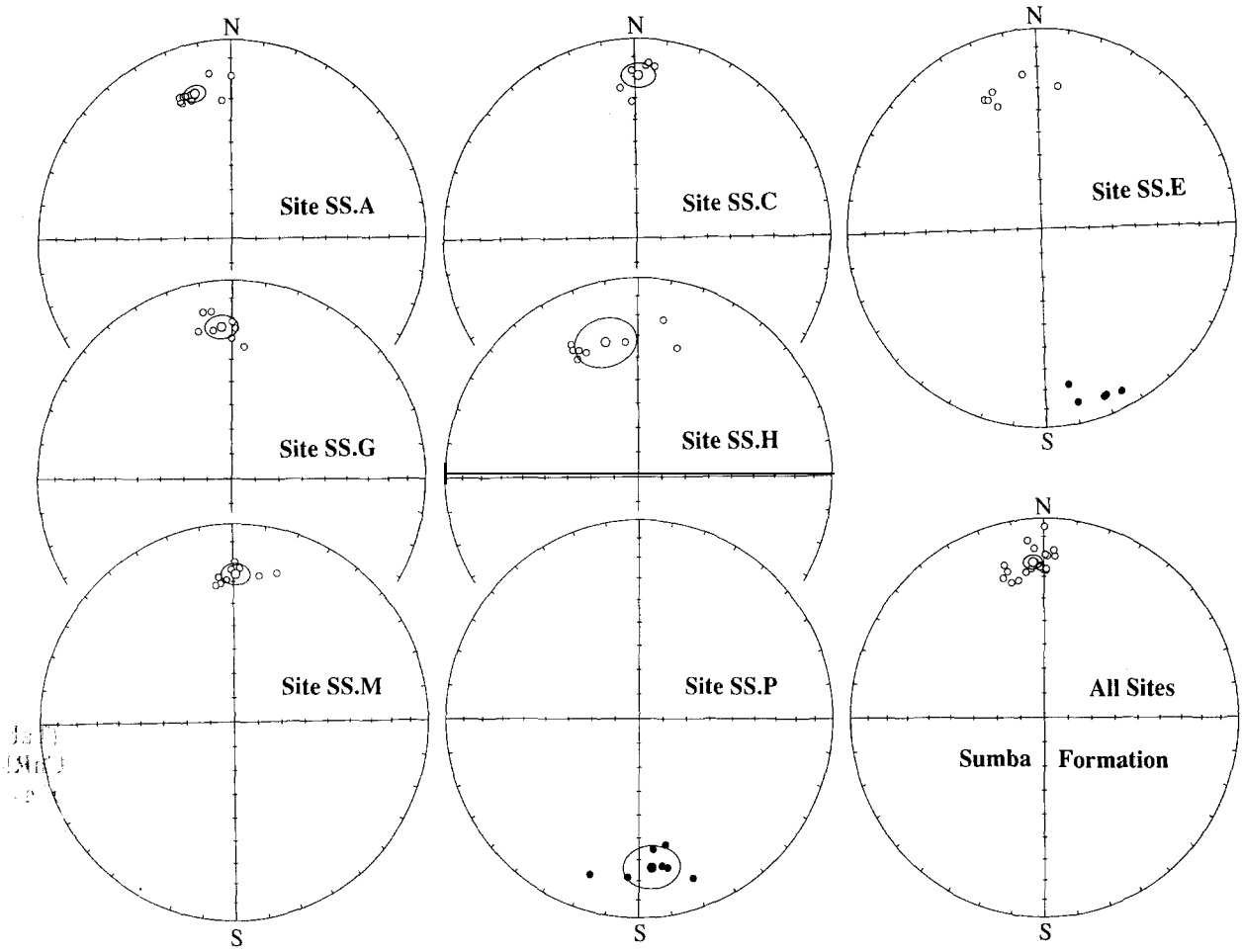

Fig. 7. Equal area plots showing the characteristic remanence directions of specimens from 7 sites from the Kananggar Formation, as well as the mean directions of all sites that were included in this study. Each projection is provided with the mean value, and with the 95% oval of confidence. Closed and open circles denote downward-pointing and upward-pointing directions, respectively. Correction of the bedding plane has been applied. See Fig. 3B for site locations.

increase of the susceptibility after treatment of 1.5–5.6%. A major increase of X with a mean value of 13% is seen after heating at 380°C (Table 2), indicating that thermal alterations must have taken place.

Lute Neogene motion history

The Characteristic Remanence directions (ChRM) of individual specimens sampled from different localities in the Kananggar Formation (Fig. 3B) are shown for 7 individual sites (Fig. 7). The equal area diagram for all the sites shows the consistency of the results. The mean ChRM directions derived from the individual sites, as well as from the combined sites are listed in Table 2. The corresponding paleomagnetic pole position derived from the mean ChRM direction, is at 85°N, 3°W and gives a palaeolatitude of 12" South (Table 3).

The data suggest that since the late Miocene, Sumba performed a small counter-clockwise rotation of some 5 degrees only. This result is slightly different from a paleomagnetic study of the Jawila Formation from western Sumba (Wensink and Van Bergen 1995); N.B. these andesites have recently been dated at 37 Ma, and are therefore late Eocene' thus probably are not E. Miocene as reported in the paper, which indicates a palaeolatitude of 11 and a possible small clockwise rotation of Sumba between this period of volcanic activity and the deposition of the Kananggar sediments. In combination, the results suggest that from the late Eocene to the early Pliocene the island was located

Table 3. Paleomagnetic pole position and paleolatitude derived from the mean characteristic remanence direction for all sites

Site	Coordinates		Pole		Position			
Lat. S	Long. E	N	Lat.	Long.	dp	dm	Palat.
9.75	120.20	21	85.4 N	2.6 W	I.9	3.6	II.87 (S)
9.75	120.20	23	85.2 N	3.7 w	2.0	3.8	II.87 (S)

N is the number of sites included in the final analysis; dp and dm are the semi-axes of the 95% oval of confidence; Palat. is the Paleolatitude in degrees.

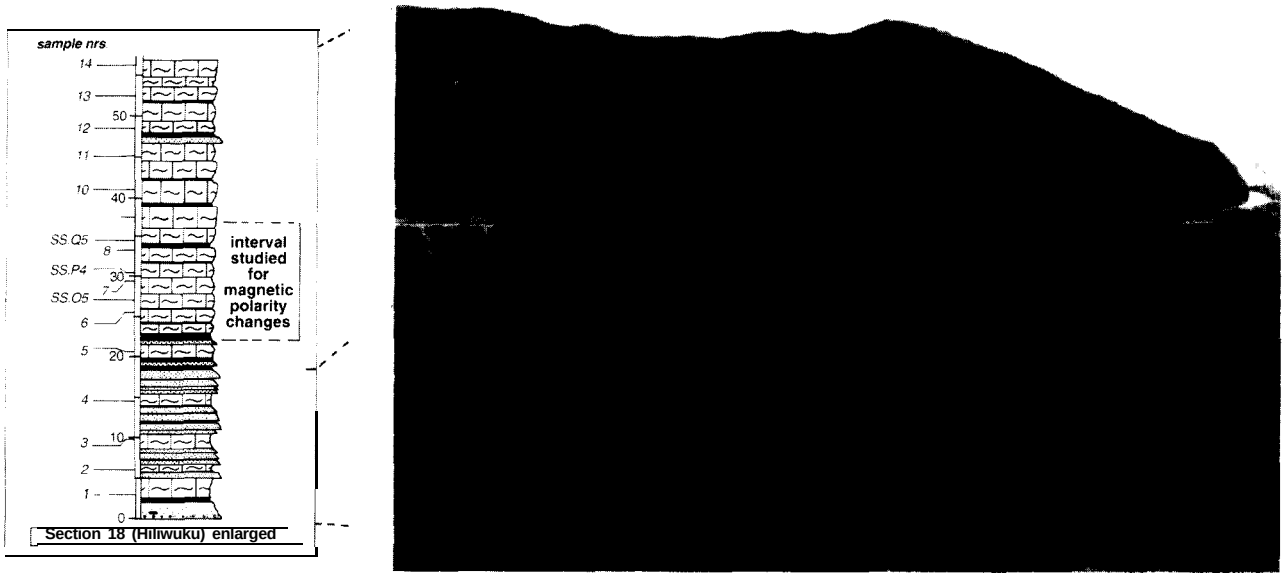

Fig. 8. Photograph and lithological column of Section 18, Hiliwuku, showing the transition from the volcaniclastic fan deposits of unit D to the pelagic sediments of unit E, sampled for magnetostratigraphy at the road level. The lithological column only indicates the micropaleontologically investigated samples. For location and position of the paleomagnetic samples, see Figure I 1.

slightly more to the south. This small northward drift probably resulted from the incipient collision between the Australian continent and the arc/trench system (Audley-Charles 1985).

Polarity reversals and the Mio-Pliocene boundary

Introduction. When the Miocene-Pliocene boundary is identified in low latitude areas on the basis of combined nannoplankton and planktonic foraminiferal data, a misfit is often noted (Fortuin *et al. 1990;* Berger et *al.* 1993; Chaisson and Leckie 1993). According to the astronomically tuned polarity time scale (Hilgen et *al.* 1995; summarized in Berggren *et al.* 1995b) the age of the M-P boundary is 5.33 Ma, and is located in the upper part of Chron C3r (Fig. 9). With regard to the presence on Sumba of pelagic sediments with good magnetic properties and the limited data for high latitude areas on the correlation of biozones with magnetostratigraphy, the possibility to use the upper Neogene sediments of Sumba has been tested. The section investigated is formed by fresh road outcrops near Hiliwuku (Section 18, Transect II; Fig. 8), at a level considered to include the Miocene-Pliocene boundary. Careful lateral bed to bed correlation of these outcrops, permitted sampling of a 13 m thick interval (a combination of sites SS.H,I,G,O,P and Q; Fig. 9). Only site SS.F, located beyond a fault, could not be correlated with this succession. In total 25 chalk beds were counted and most of them were sampled.

Results. In general, normal polarities are more commonly observed in the Kananggar Formation (Table 2). Only site SS.P of the Hiliwuku section reveals ChRM directions of reversed polarity, whereas site SS.E (Figs 2, 7) shows both normal and reversed ChRM directions. Reversed directions of magnetization cannot always be detected, because specimens with a primary reversed polarity may have been overprinted in a magnetic field of normal polarity with the same orientation but opposite polarity. Remagnetization may occur both during normal and reversed periods of magnetic polarity. Some of the specimens of sites SS.P and SS.Q with small initial remanence intensities (Table 1) revealed large viscous components of magnetization. During progressive demagnetization, these specimens showed a rapid decrease in remanence intensity, and made it difficult to isolate the (reversed) ChRM direction. However, the majority of the specimens, except those from sites SS.P and SS.Q, reveal reliable paleomagnetic data with ChRM directions of both normal and reversed polarity.

The investigation started above the last major turbidites in unit C, around the first occurrence of *Globorotalia tumida*. The first appearance of this species provides a means to denote the base of Biozone P11 at a level close to, but slightly older than the base of the Pliocene (Berggren et *al.* 1995a). In the concept of Srinivasan and Kennett (1981) the first appearance of *G. margaritae,* which usually appears somewhat above the first appearance of *G. tumida*, is a reliable indicator for the base of the Pliocene in the Pacific and e.g. observed on the Ontong-Java Plateau, but

Fig. 9. Stratigraphic column of the successive paleomagnetic sampling sites SS.G, SS.O, SS.P, and SS.Q; the sections of the sites SS.H and SS.I are given together with their possible correlation in the lower part of the main column. The palaeomagnetic polarities (N and R) are given; reliable data, usually based on the results of three or more specimens, are given in bold (R and N). The most likely correlation of the lower part of the section with the geomagnetic time scale covering the latest Miocene and very early Pliocene is shown to the right (after Cande and Kent 199.5). The age of the Miocene-Pliocene (MPB) boundary is indicated after Hilgen and Langereis (1 993). The sketch map at the bottom shows the location of the paleomagenetic sampling sites.

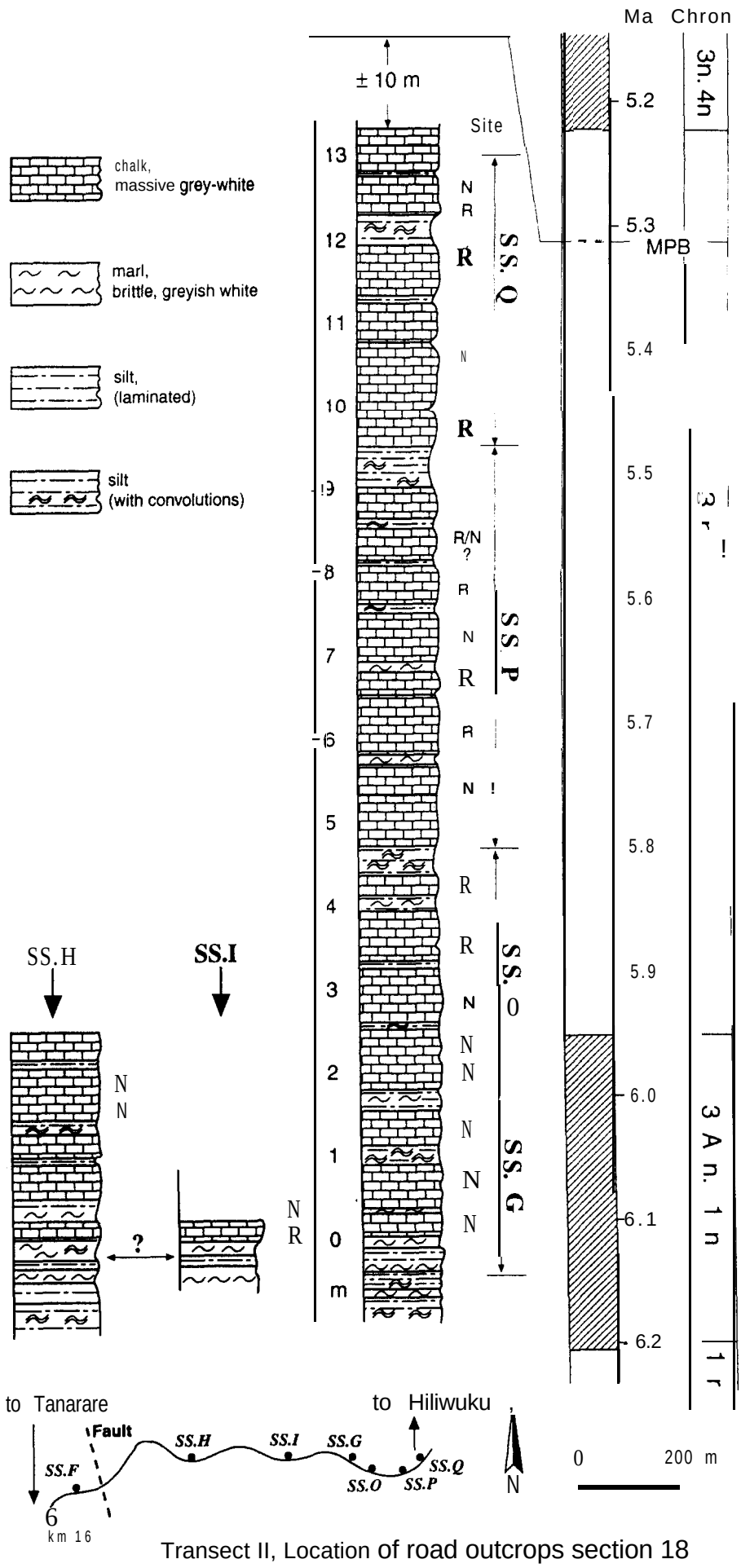

Transect II, Location of road outcrops section 18

Figure 9. Caption on facing page.

according to others its first occurrence is rather erratic.

The geomagnetic polarities (N, R; indicated in Fig. 11 in bold face) are considered reliable, as they are based on identical results from three or more specimens. The sampled interval begins with a bed with a R polarity (site SS.I), overlain by a 3 m thick sequence with N polarities. Then follow R polarities with some intercalculated N polarities, which are considered to be overprinted R polarities. If not, these N polarities would represent virtual N polarity intervals. This, in turn, would mean that such intervals have a thickness of only one or two layers. As discussed later, the average accumulation rate of the late Miocene-early Pliocene chalks is in the order of 0.036 mm/a, a common rate for deposits of this age and kind (Berger and Stax 1994). A one meter interval then represents too short a period of time to account for a polarity chron. Moreover, no short normal geomagnetic polarity events have been reported within the reversed Chron C3r. Therefore, we accept that the intercalated N polarities in sites SS.P and SS.Q were originally R polarities.

Concluding, it is most likely that the observed main N–R polarity transition represents the base of the Gilbert Chron, and the underlying N interval corresponds to the upper part of Subchron C3An.1n. The main reason for this conclusion is the presence of G. *tumida* at the base of section 18, and the first occurrence of *G. margaritae* in sample SS.O5. According to Berggren *et* al. (1995a) the former species appears during C3r, at 5.6 Ma, but with an inferred possible earlier occurrence during Subchron C3An. 1 n, i.e. around 6 Ma. Because this species appears in our material (sample 18-1, Fig. 8) below as well as above the N–R polarity reversal, it is unlikely that this is an even older reversal. If it marks the next younger reversal from C3n.4n to C3n.3r (at 5.0 Ma in Berggren et al. 1995a, b), that level should be above biozone NN 1 lb. This stratigraphic level could be ruled out, because all samples of this section, excluded the uppermost one, still contain late Miocene calcareous nannofossils (the assemblages consist of at least *60%* of *Eudiscouster quinqueramus/berggrenii*, i n association with *Amaurolithus primus*).

The early occurrence of *G. tumida* strengthens the assumption of Berggren *et al.* (1995a) that its entry already may have taken place during Subchron C3An1. 1n, although this species is uncommon until a level within the reversed interval (common in SS.Q5, Figs 10, 11). Until then, the samples rather include *G. plesiotumida*, *G. cibaoensis*, plus *G. menurdii* and *G. pertenuis.* The absence of *Globoquadrina dehiscens* confirms the observation of Chaisson and Leckie (1993) that this species appears much later in the region.

Thus, most of the sampled interval can be correlated with the lower Gilbert Subchron C3r. Within this Subchron the M-P boundary is situated close to the transition to C3n.4n (Thveri), which boundary is now established at 5.32 Ma (Baksi 1993; Hilgen and Langereis 1993), or, following the most recent calibration, at 5.33 Ma (Lourens *et al. 1996).* Because the Pliocene Epoch starts 0.62 Ma later than the base of the Gilbert Chron (Fig. 9: base C3r), the **M-P** boundary could be located approximately 20 m higher up in the section (or 10 m above the top of the section of Fig. 9), applying the possible sediment accumulation rate of 0.036 mm/a. Thus the M-P boundary is probably positioned above the magnetostratigraphically investigated interval, but also very likely below the first sample containing a Pliocene nannofossil assemblage (only the uppermost sample 14 of section 18, Fig. 8). Despite just missing the transition to C3n.4n and so the exact location of M-P boundary, the emplacement of this section in the magnetostratigraphic time scale was successful.

Onshore-offshore correlation

Offshore seismic stratigraphy

Seismic modelling of outcropping sediments aids in bridging the gap between the low resolution of seismic profiles and the detail of the geologic sections (Stafleu 1994). If transformed that way, the volcaniclastic submarine fan deposits of Sumba may serve as a reference section for interpreting multi-channel seismic profile Pat-109 (Figs 2, 10). Because the uplifted southern faultblock of Pat-109 is situated along-strike from the basement high forming the Massu Mountains, of which the Neogene cover has been removed since its emergence, correlation seems evident. However, the considerable lateral distance prevents a direct correlation of the lithologies.

The evolution of a volcaniclastic submarine fan system, distributed over both the Sumba Ridge (van der Werff 1995a) and the island of Sumba, will be related to activity of a middle-late Miocene volcanic arc. As the average stratovolcano has a basal diameter of 30 km (Suga and Fujioka 1990; Walker 1993), the sediments deposited on East Sumba and in the western Savu Basin will in such a case originate from different individual volcanoes. Thus the resulting seismic units may have been deposited during and after different eruption events, at different rates.

The seismic stratigraphy of Pat-109 (Van der Weff 1995a; Fig. 10) consists of 4 seismic units, which characterize much of the Savu Basin stratigraphy:

Seismic Unit 1. This unit is only locally present on top of the northern basement blocks, where it reaches a thickness of 0.6 sec. TWT. The lower part (1A; Fig. 10) is characterized by chaotic, discontinuous high amplitude reflectors, overlain by transparent to weakly reflective beds. Both the external form and reflection pattern of the lower reflectors suggest the presence of reefal mounds, that formed at the edge of the basement blocks. The transparent facies above (subunit 1B, Fig. 10) could represent marls that were deposited in a more restricted environment. The mounds correlate with the Paleogene carbonate platforms of Sumba.

Seismic unit 2. This unit is composed of a large sequence of northward prograding, continuous, moderate to high amplitude reflectors that downlap the basement and seismic unit 1. Progradation over 100 km is indicated. The unit has a maximum thickness of 1.4 sec TWT (- 1700 m) and the reflectors have an average slope angle of $\sim 3^{\circ}$. The oldest reflectors (subunit 2A) are up to 1.4 sec TWT thick (Fig. 10, part 1). Its top is truncated by a high amplitude reflector that may represent a major erosional unconformity.

Subunit 2B is represented by base of slope mound deposits that have a thickness of 0.25 sec TWT. The

deposits partly overlie Unit 1 and partly onlap Subunit 2A. The lower half of the mound is characterized by fairly continuous high amplitude reflectors that are covered by a more transparent seismic facies unit. To the south, subunit 2B consists of a major slide mass, situated on the edge of a fault block (Fig. 10; shotpoints 5400-5700). The strata show an undulating pattern of medium amplitude reflectors that onlap subunit 2A and passing downslope into moulded, chaotic seismic facies.

Subunit 2C comprises a sequence of prograding, continuous, medium to high amplitude reflectors with a thickness of 0.30 sec TWT that downlap subunit 2B. The top of the unit is truncated by the base of subunit 2D.

Subunit 2D consists of a third sequence of prograding, continuous, high amplitude reflectors that are deposited more basinward. It has a thickness of 0.25 sec TWT and is onlapped at its base by seismic unit 3.

Seismic unit 3. This is a sequence of fairly continuous, medium amplitude reflectors that slightly onlap Unit 2. Based on its seismic reflection characteristics, the unit presumably correlates with the upper part of the Kananggar Formation, which consists of an alternation of variably resistant Pliocene chalks and marls.

Seismic unit 4. This unit has locally been eroded by bottom currents. It represents a basin fill unit that laps on to Unit 3 and is composed of continuous high amplitude/low frequency reflectors. It reaches a maximum thickness of 0.5 sec. TWT ($\sim$ 600 m).

Synthetic seismic section

The procedure for obtaining the synthetic seismogram of Transect II (Fig. 11) is described in Van der Werff (1996). who applied the methods developed by Stafleu (1994) and Stafleu and Sonnenfeld (1994). The petrophysical data (Table 4) on which the seismogram is based were obtained following the procedure given by Kenter *et al.* (in press). The stratigraphical position of these samples from Transect II is indicated in Fig. 3. Because the 30 m thick chalky upper Unit E (Section 18; Fig. 3) represents only part of the entire chalky Pliocene succession, this lithology has been extended to 130 m, as an approximation of the minimum amount deposited prior to erosion after emergence of Sumba. Of the two modelled frequencies, the broad low-frequency 25 Hz wavelet provides the synthetic seismogram that can be best compared with the resolution of multi-channel seismic profile Pat-109. The higher frequency 50 Hz wavelet provides comparable, but more pronounced divisions of the seismic facies.

Three seismic facies can be distinguished in the synthetic seismogram (Fig. 1 1). The lower 0.2 sec TWT comprise an alteration of widely spaced high amplitude reflections that correspond to the volcaniclastic turbidite/debris flow deposits of lithostratigraphic Units B-C. These are followed by 0.1 sec TWT of relatively closely spaced high amplitude reflections that relate to the thicker and more regularly bedded turbidite/debris flow deposits of Unit D. The upper 0.15 sec TWT consist of a transparent zone that correlates with the pelagic chalks of Unit E.

The condensed marly base of the Kananggar Formation (Unit A), is represented by a negative high amplitude reflection event and cannot be resolved as an individual seismo-stratigraphic unit. The thick turbidites of unit B and the lower part of unit C are resolved as one prominent high amplitude reflector. The thick-bedded, coarse grained debris flows and turbidites of units C and D have high P-wave velocities and bulk-densities (Table 4) generating high amplitude reflections. Due to constructive interference, closely spaced turbidite beds will be resolved as one reflection event, but not on the 50 Hz seismogram, where the major debris flow units and sandstone turbidites with a minimum thickness of 5-10 m are resolved as separate high amplitude reflections. Relatively low impedance contrasts result in unit E, where distal turbidites, silts, foraminiferal oozes and chalks all have moderate bulk-densities and P-wave velocities (Table 4). Consequently, these lithologies are not resolved on the synthetic seismogram as individual units.

On the 25 Hz seismogram, the entire 30 m alteration of thin turbidite beds and hemipelagic clays in the middle part of unit C (at 0.50 sec TWT) is resolved as one high amplitude reflection due to constructive wave interference. At the top of unit C, at 0.40 sec TWT, a similar lithology has, however, resulted in a very low amplitude event, in this case probably the result of destructive wave interference. Such interference processes disturb the identification of both fining/thinning-up and upward coarsening/thickening turbidite cycles.

Fit of synthetic seismogram and seismic profile

Transect II (Fig. 3) represents a complete but still rather "condensed" section of the Kananggar Formation with regard to the eastward trend of increasing significance of the volcaniclastic interbeds. Comparison between the 25 Hz synthetic seismogram and multi-channel profile Pat-109, suggests a correlation between the high amplitude wavelets of units B, C, D and seismic unit 2, and between the low amplitude wavelets of unit E and seismic unit 3. Profile Pat-109, shows four successive phases of submarine fan progradation of which Fig. 14A mainly presents the youngest unit 2D. The fit with this succession is good.

The most complete vertical seismo-stratigraphic section is located along strike from the Massu Mountains. This part of profile Pac-109 (Fig. 10B) shows all the identified subunits of Seismic unit 2, but has an estimated thickness of 800 m and therefore fits less well. The presence of north-dipping reflectors (Seismic unit 2A), a large submarine slide (Seismic unit 2B), and the low amplitude northward prograding reflectors (lower part of Seismic unit 2C) compare better with onshore Transect III (Fig. 3).

Another good offshore analogue of the Transect II section is located north of a major fault (Fig. 12C), which delimits the offshore northern margin of the Massu mountains (Fig. 2B; SP 5700). Seismic unit 1 correlates with the tilted Eocene carbonate platform, seismic unit 2B with the turbidite wedge complex (Unit B), seismic unit 2C with the turbidites of sequence C-1 and seismic unit 2D with the upper distal part of unit C and the coarse clastic suprafan lobe deposits of Unit D. Seismic unit 3 correlates with the early Pliocene chalky strata of Unit E. If correct, a difference would be the thicker developed portion of unit 2D.

Although seismic unit 2 is thicker (0.67 sec TWT, or $\sim$ 880 m), we suggest the following correlation: the high amplitude reflector at the top of Seismic unit 2B correlates with the prominent reflection generated by the

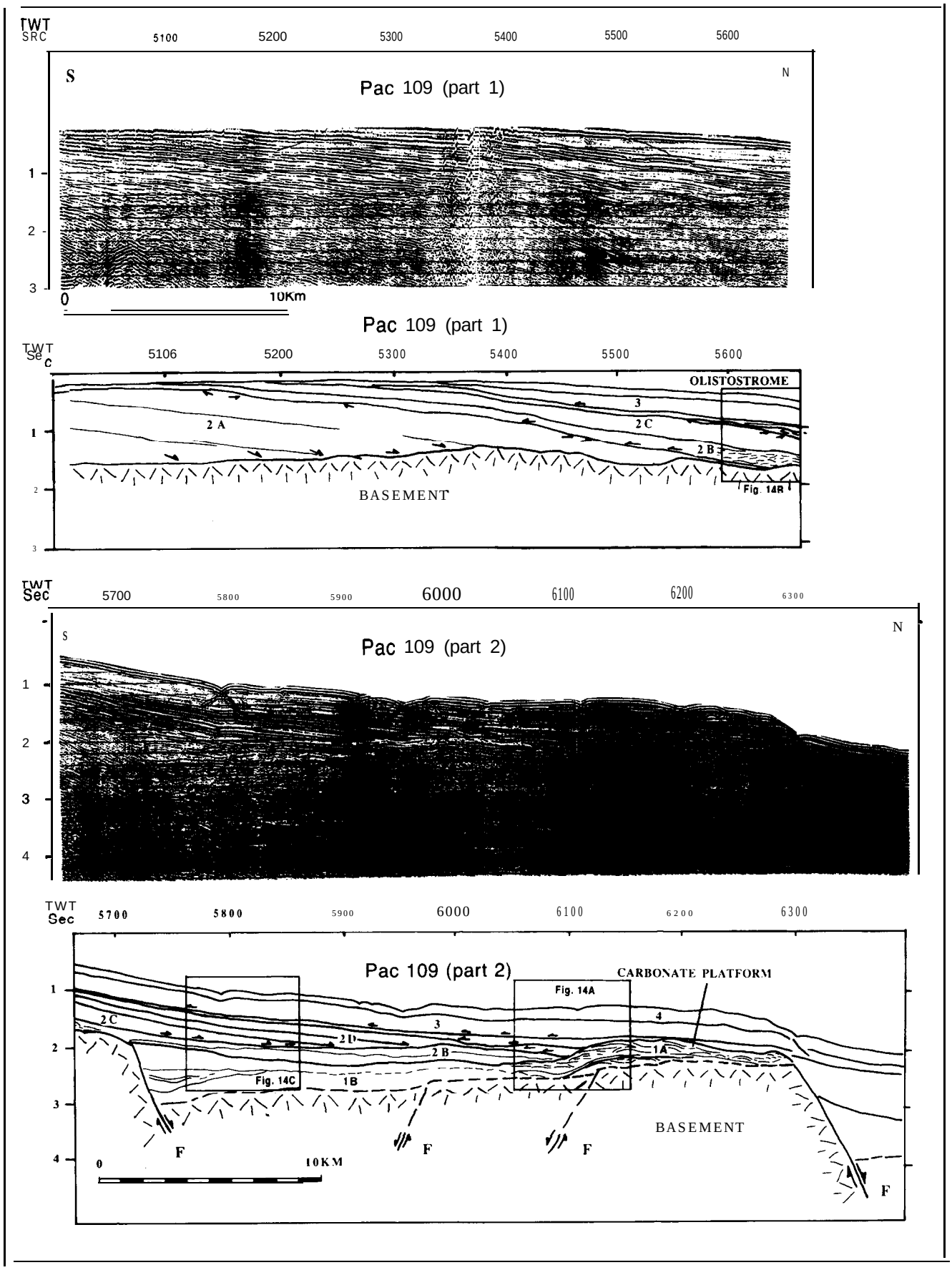

Fig. 10. Seismic profile Pat-109 (Parts 1 and 2) between shotpoints 5000-6400 with line drawn interpretation. For location, see Fig. 3A. The profile shows a sequence of northward prograding high-amplitude reflectors deposited on top of a faulted basement (unit 1), and covered by onlapping semi-transparent reflectors (unit 3). The interpreted section shows the geometry and internal structure of this interpreted prograding volcaniclastic submarine fan system. 4 Seismic sub-units (2A–D) define its internal geometry. The insets represent parts that are compared with the synthetic seismogram generated for Transect II (Figs 13. 14).

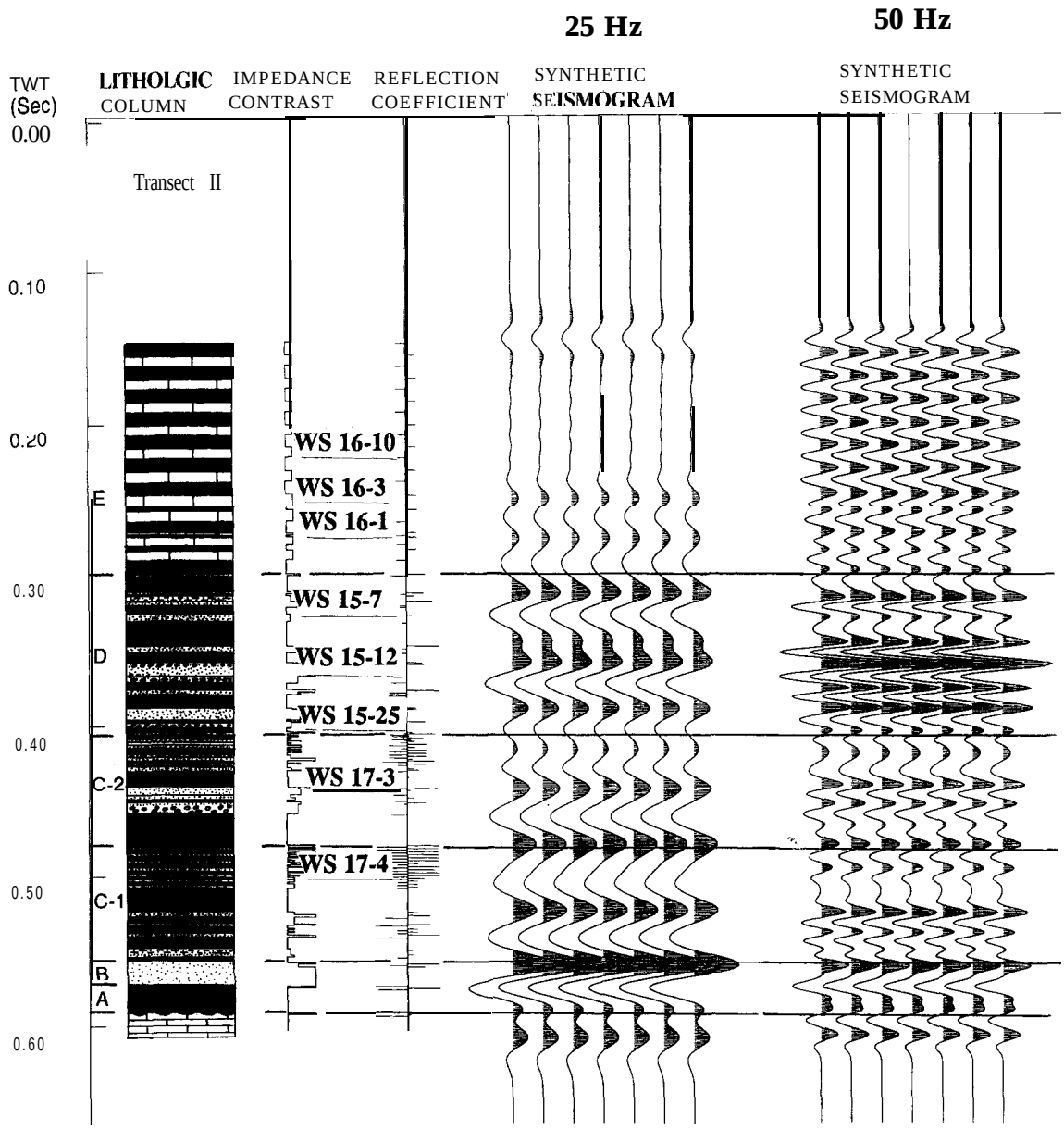

Fig. 11. Converted simplified lithologic time section of Transect II, along with impedance contrast, reflection coefficient and 25 Hz and 50 Hz synthetic seismograms, made using the vertical incidence modelling program VERTINC (Stafleu 1994). Positive reflection events are indicated in black. Each seismic trace is repeated 7 times. The horizontal lines mark the member boundaries on the synthetic seismogram.

turbidite complex of lithologic Unit B, Transect II. The two high amplitude synthetic reflections generated by the fan deposits of lithologic units C-l and the base of C-2, Transect II, correlate with seismic unit 2C. The transparent interval related to the more distal fan deposits of lithologic unit C-2, Transect II correlates with the transparent zone of the lower part of Seismic unit 2D. The 3 high amplitude reflectors situated above the transparent zone may correlate with the upper part of Seismic unit 2D.

It is concluded that construction of a one-dimensional synthetic seismogram of the Kananggar Formation enables the recognition of its major stratigraphic units as characteristic seismic facies, which can be related to units represented in offshore profiling. Thus the hypothesis that the onshore submarine fan deposits can be correlated to the record on Sumba Ridge is accepted. The increase in sediment thickness from 600 m near Transect II, to 1.7 km east of Sumba, indicates that the offshore part formed a main depocenter. The probable offshore extension of the volcaniclastic facies (Fig. 13A) is substantial: all over Sumba Ridge, where the succession is southward cut off by the Savu thrust, towards the deeper parts of the south Savu Basin (see seismic profile Rama 83, Fig. 13, Van der Werff *et al.* 1994). A model of the possible lateral facies development across the correlated and differentially subsided sections is given in Fig. 13B.

Discussion

Geohistory

The angular unconformity between the Paleogene platform carbonates and the overlying Neogene succession is considered to represent a break-up stage preceding the overall subsidence of Sumba. Abundant

Table 4. List of the samples of Transect II analysed for petrophysical properties, classified according to their lithology. The sample positions are indicated in Fig. 3. The measured properties are carbonate content (%), bulkdensity (g/cm'), *P-wave* velocity (km/s) and porosity

Sample number	$CaCO_3$ (%)	P_s (g/cm')	V_p (km/s) Pe = 5 MPa	Nt (%)
Pumiceous debris flow				
WS 15–25	38.90	1.69	2.50	52.35
Coarse volcaniclastic sandstone (250–1000 μm)				
w s 15–7	29.60	2.71	3.56	22.33
WS 16–1	42.50	2.14	2.67 ,	28.88
Fine volcaniclastic sandstone (64–250 μm)				
WS 16–3	33.20	1.96	2.18	41.64
WS 15–12	23.20	1.68	2.03	57.10
Silt (2–64 μm)				
ws 17-3	28.10	1.66	1.88	56.05
Chalk (Foraminiferal Ooze)				
ws 174	57.80	1.67	2.00	55.91
w s 6–8	69.80	1.78	2.1 1	46.98
w s 1–3	65.20	1.95	1.90	50.68
w s 1–4	70.00	1.57	2.17	53.13
ws 1-9	79.00	1.67	2.25	59.13
Clay/Marl				
WS 16–5	57.70	1.66	1.83	56.39
WS 16-10	50.20	1.88	2.12	41.94

reworked Oligocene and Cretaceous calcareous nannofossils at the unconformity suggest considerable erosion of the underlying units. On central Sumba bathyal-abyssal environments were not established before the late Miocene, whereas further east CCD depths were already reached during the middle Miocene. Differential subsidence along NE-SW directed basement faults did play a role, as suggested by fault zone F1 (Fig. 2) which separates the turbidite poor sequences of central Sumba from the volcaniclastic successions of East' Sumba and their offshore equivalents. Presence of middle Miocene volcaniclastic fan deposits also to the south of the Massu mountains and the likely presence of coeval fan deposits along-strike further offshore (Fig. 13A), underscores the regional importance of these middle Miocene tectonic changes in which the main depocentres probably were located offshore. The volcanic sources of island arc character, which supplied the volcaniclastics were located S of Sumba, as shown onshore by dominantly NNE directed paleocurrents and, offshore, by the over 100 km northward prograding fan morphology. Volcanic activity probably controlled the basinward transport of its ejecta and reworked bioclasts of near-shore origin towards a progressively subsiding proto Sumba-Savu basin. The large W-E, or WNW–ESE lateral distribution of the volcaniclastics (Fig. 13A) suggests that this proto Sumba-Savu basin had a similar orientation.

The age and depth data of the condensed basal unit A indicate that East Sumba subsided at least 3 km during the Middle Miocene (Langhian-Serravallian). Subsidence started near the beginning of the Middle Miocene (or ~ 16 Ma) and the CCD level was reached before the end of biozone NN6, or before 12 Ma. In the geohistory diagram (Fig. 14), a depth of 4.5 km is indicated for the average depth of the CCD (Kennett 1982). With open marine sedimentation not before 15 Ma (adopted in Fig. 14 is an arbitrary depth of 1000 m at that time) and CCD influence evident from ~ 12 Ma an average rate of subsidence of slightly more than 100 cm/ka is suggested. Such a high rate can be expected in case of syn-rift subsidence (Pitman and Andrews 1985). According to the latter authors fast initial rift subsidence commonly results in initial sediment starvation, which feature was recognized for unit A. A similar subsidence rate is indicated during Miocene intra-arc rifting in N Japan (Yamaji 1990; lngle 1992).

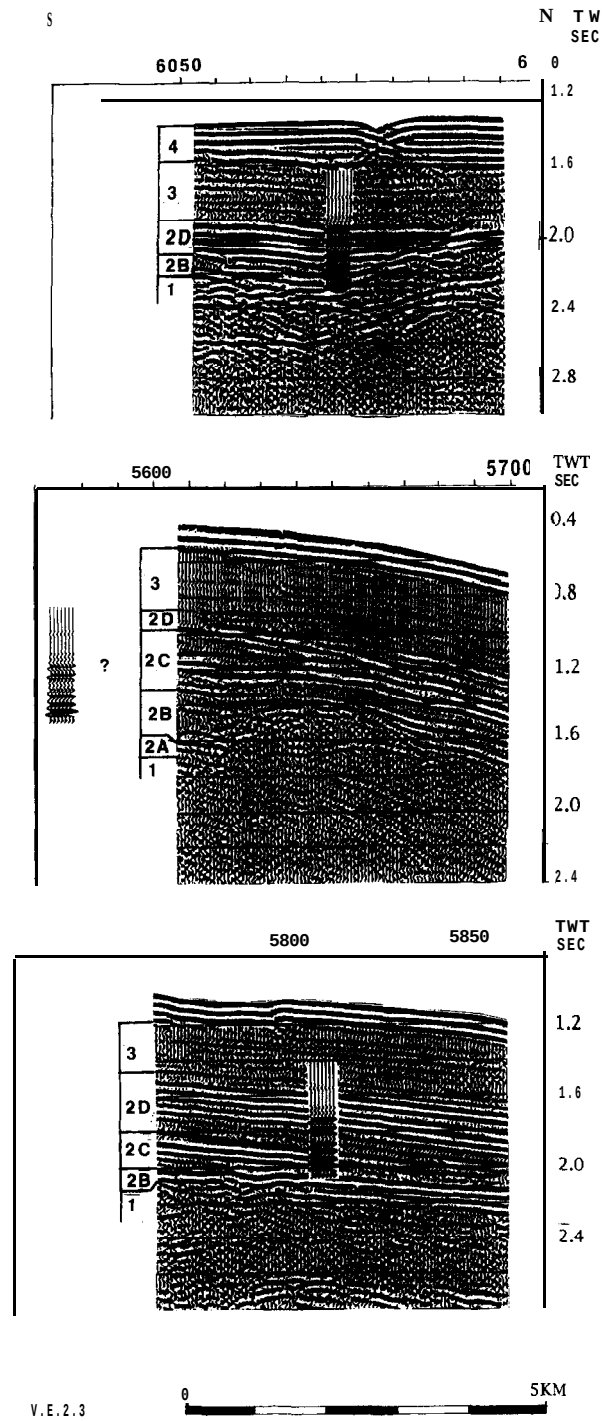

Fig. 12. Correlation of the synthetic 25 Hz seismogram with various parts of seismic profile Pac-109. A, Between SP 6050–6150. B, between SP 5600–5700. C. between SP 5700-5860

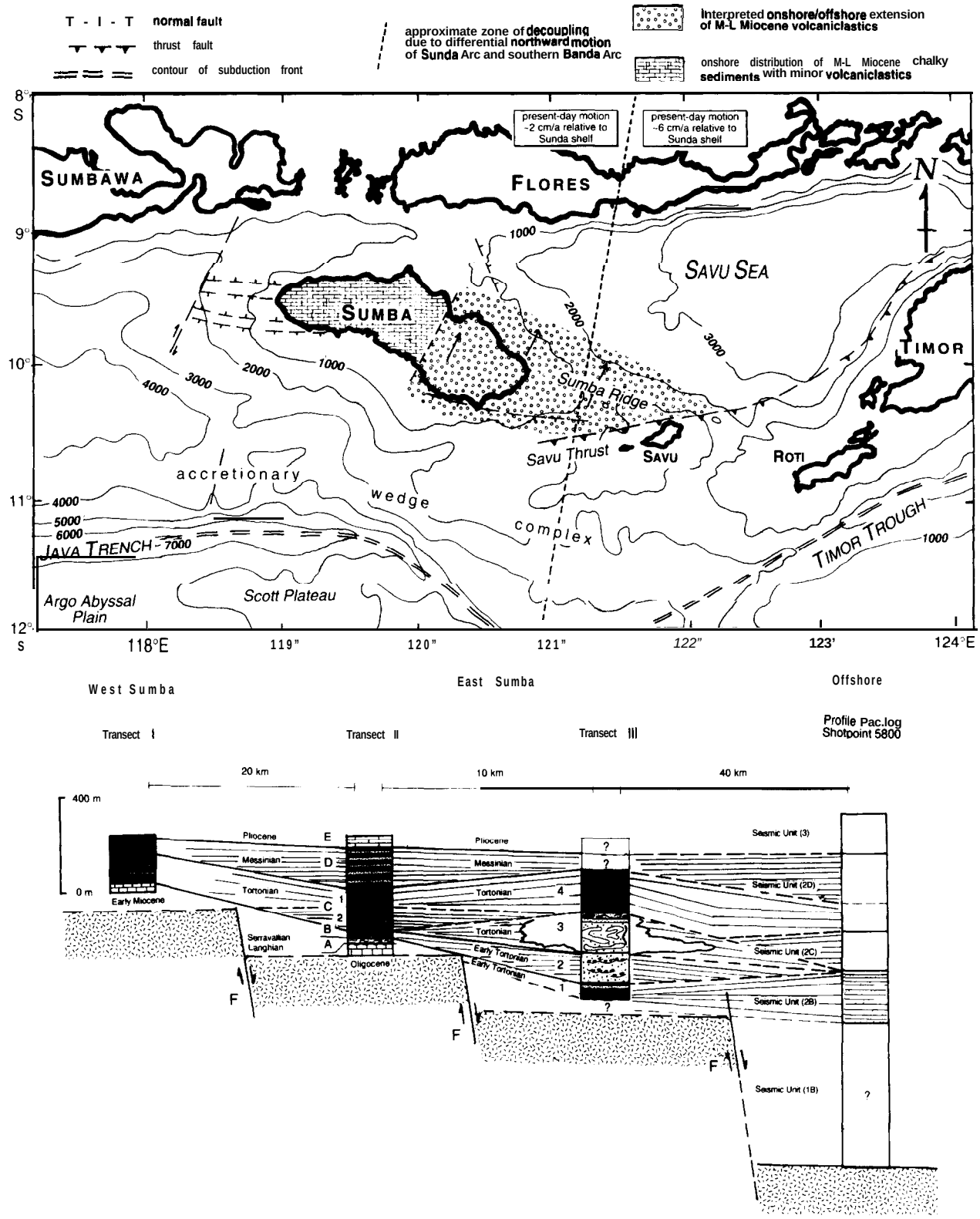

Fig. 13. A Map of Sumba and surrounding basins, showing the 1000 m isobaths (after Pertamina/BEICIP I :2.000.000 map of eastern Indonesia, 1982) and actual morphotectonic aspects with regard to greater Sumba (simplified after Van der Werff 1995). Added are the interpreted extent of the middle-late Miocene deep water volcaniclastics and their lateral. more chalky equivalents onshore. The arrows indicate the inferred main paleocurrent directions. Also indicated are rates of present day crustal motion (after Genrich *et al.* 1996). B Model showing the possible lateral facies patterns between the differentially subsided and chronostratigraphically correlated onshore transects and the offshore seismic units of Pac 109 at shotpoint 5800. See Fig. 2 for location.

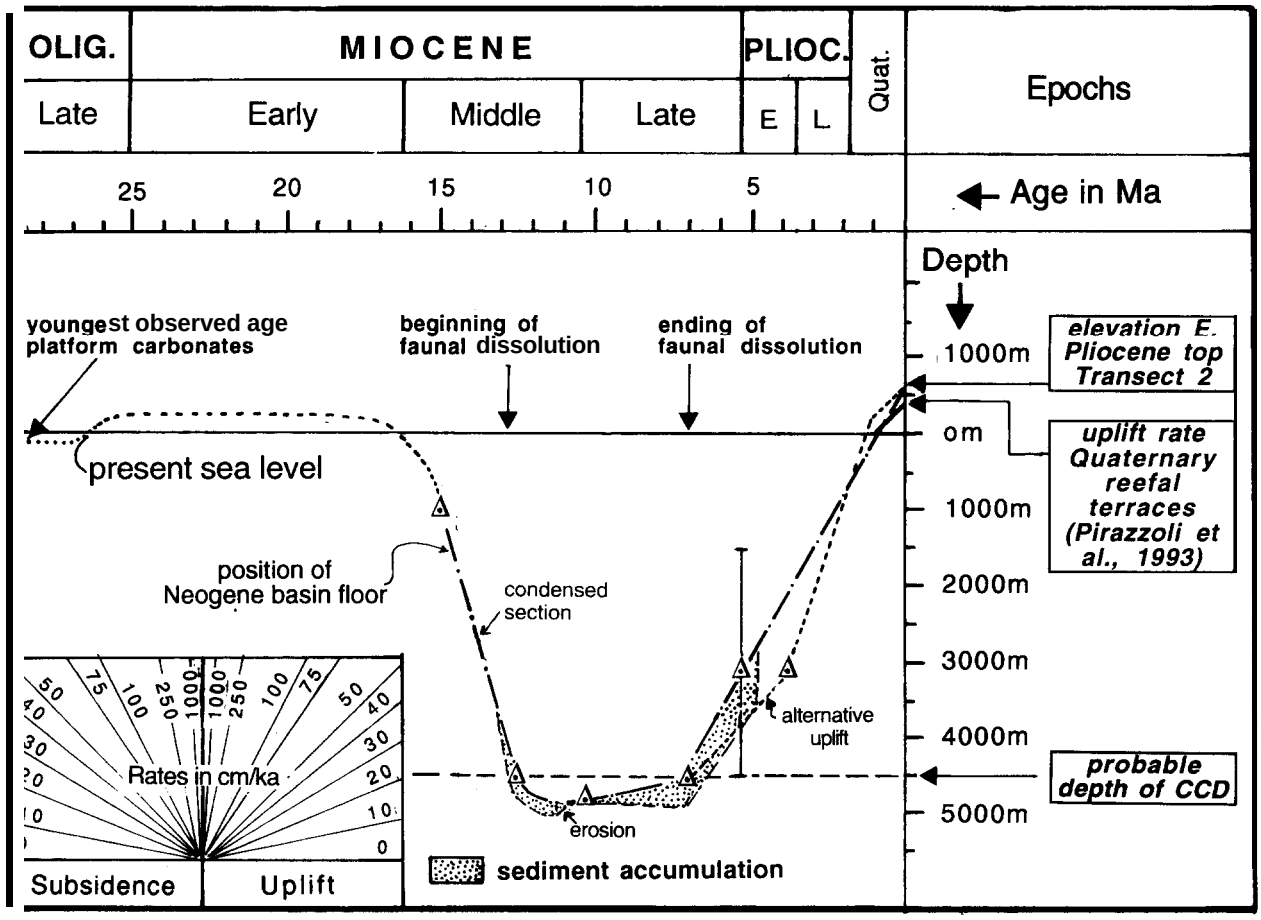

Fig. 14. Geohistory diagram for the Neogene deposits of East Sumba, based on Transect II. Sealevel is considered as if constant (eustatic variations being an order of magnitude smaller than the vertical movements involved). The horizontal axis gives age in Ma. Triangles indicate the interpreted depth (or centre of depth range) during the dated depositional intervals. For the depth of the CCD the average of 4500 m has been adopted (Kennett, 1982). The present depth of the CCD in the Argo Abyssal Plain is around 5400 m (Adisaputra, 1989). The total amount of Middle Miocene sediment accumulation is uncertain. due to poor onshore exposure.

Calcareous nannofossils still present within the CCD-affected intervals indicate that depths probably did not exceed ~ 5 km. This suggests that during the supply of the most of the volcaniclastics subsidence has decreased considerably, which could be an effect of transition from fast mechanical subsidence to thermal subsidence. The first indications for shallowing of East Sumba come from the gradual reappearance of foraminiferal assemblages in Transect II during the Messinian. The absence of any regional unconformity at this level and the gradual upward change suggest, however, that the rise above the CCD level may mostly have been an effect of basin infilling (apart from possible fluctuations in the depth of the CCD). The general termination of volcaniclastic supply just prior to the Mio-Pliocene boundary indicates changing basinal conditions, coupled with overall uplift. At the beginning of the Messinian (~ 7 Ma ago) basinal depositional depths were still below the CCD, but soon rose above this level. With these deposits at a present altitude of 600 m at the top of section 18, an average rate of uplift of 0.73 mm/a is suggested for that section. However, uplift may not have been linear. An alternative, also indicated in Fig. 14, is based on Pleistocene uplift of 50 cm/ka as calculated from the dating of reefal terraces up to 1 Ma in age in the coastal area (Pirazzoli *et al.* 1993). This lower Quaternary rate thus implies faster uplift, of ~ 100 cm/ka during the late Pliocene. Another reason to assume faster uplift during the late Pliocene is the finding of deep water foraminiferal chalks dated as approximately 3.8 Ma in Central Sumba. These indicate that, if uplift was already going on there since the early Pliocene, it cannot have been significant. Because major phases of uplift will have affected both regions at the same time, this alternative scenario of faster uplift after 3.8 Ma is also indicated. Even a rate of 100 cm/ka is an order of magnitude smaller than the fastest uplift calculated for Plio-Pleistocene uplift in Timor (De Smet *et al.* 1990).

The almost turbidite free latest Miocene part of Transect I (Section 24, Rambangaru) could be relatively well dated, thus permitting an estimate of the average rate of pelagic sedimentation. Zone N 17 (duration 2.7 Ma, Berggren *et* al. 1995a) comprises at least 97 m of sediment, which indicates an average sediment accumulation rate of ~ 0.036 mm/a. This figure agrees well with the late Miocene sedimentation rates of pelagic chalks reported from the Ontong Java plateau (Berger and Stax 1994). As can be expected, the accumulation rates of the late Miocene, in the volcaniclastic poor and rich Transects I and II, differ considerably. With a duration of up to 5 Ma for approximately 300 m of sediments in Transect 1. this

amount is somewhat higher (0.06 mm/a) than in section 24. In Transect 11 (600 m during the Tortonian), the sediment accumulation rate has been in the order of 0.15 mm/a.

Moderate faulting and a gradual northward tilt of only a few degrees in many places are the most prominent features of the uplift of East Sumba, which together resulted in a maximum elevation of 1200 m of the basement in the Massu fault block. This gradual tilt implies somewhat faster uplift of that segment than the coastal Neogene near Waingapu. Assuming that at least some 500 m of Miocene submarine fan deposits must have been eroded from the Massu uplift, plus a certain amount of basement rock, a hypothetical elevation for the base of the Pliocene would be about *2000* m. Extrapolation of that elevation with a minimum average uplift rate of 0.65 mm/a suggests that also the highest part of Sumba did not emerge before 3 Ma.

Plate tectonic significance of the volcaniclastics

Until now no relics have been found from the interpreted Miocene volcanic (proto)arc S of Sumba, as its inferred location has been faulted down along the Savu Thrust, or, more westward, has been incorporated in the broad accretionary complex, or could possibly have been subducted (Van der Werff 1995a, b). An interpretation of related plate tectonic aspects therefore has to remain tentative. As discussed in the previous section, the Sumba record reflects the sudden change to an extensional setting, resulting in rifting with strong initial subsidence during the Middle and Late Miocene, followed by a compressional regime causing uplift and emergence of large parts of the Sumba terrane. The combination of rifting and the growth of volcanic centres somewhere to the south of Sumba implies that the region became part of a backarc basin at the onset of the Middle Miocene, as suggested by Fortuin *et al.* (1994) and Van der Werff (1977). The interpretation of changing stress regimes related to island-arc tectonics is not straightforward and various models exist in literature. A major factor to cause tensional stresses in a backarc is trench rollback, which may be associated with steepening of the dip angle of the slab. In the case of Sumba, subduction of increasingly older and heavier Indian ocean crust could have contributed to this. Otsuki (1989), however, empirically showed that shortening, or extension of the arc crust mainly depends on deviation from a "standard convergence rate" of 7.2 cm/a, with lower convergence rates resulting in extension. Despite uncertainty which forces governed these fundamental changes in the Sumba region, 3 regional aspects should be considered: (a) the implication of older Sumba volcanics, (b) the developments in the Sumbawa-W Flores volcanic arc segment and, (c) the possible intereaction between the Sumba terrane and the advancing Banda arc region.

The Jawila volcanic episode of W Sumba, which traditionally is interpreted as an early Miocene magmatic event, also reflects island arc volcanism (Wensink and van Bergen 1995). However, because recent age dating indicates late Eocene magmatism (Wensink, pers. comm.) this stage has little to do with the Neogene East Sumba-Savu Basin volcaniclastics. Nevertheless, it illustrates the longstanding position of the Sumba region along the southeastern margin of Sundaland, at 11°–12°S, according to the combined paleomagnetic results discussed by the latter authors and herein. This position differs fundamentally from the juxtaposed Banda Arc segment, which drifted northward in front of Australia (Rangin *et al.* 1990), resulting in a transtensional to transpressional tectonic setting for the Sumba terrane.

In order to explain the discovered 'lost volcanic arc' that should have existed S of Sumba Fortuin *et al. (I 994)* suggested a possible link with a gap in volcanic activity in the present Sunda Arc during the Middle and Late Miocene, as documented by Barberi *et al.* (1987) for the island of Sumbawa and by Nishimura *et al.* (1981) for western Flores. More specifically, the data of these authors indicate that after volcanism had ceased during the early Miocene (after ~ 19 Ma) in the eastern part of the Sunda Arc, a condensed succession of Middle Miocene platform carbonates was formed. This platform deepened towards the south and lagoonal sediments were deposited to the north. A large hiatus indicates subsequent emersion and erosion. This depositional history suggests to us that, when this region became a dormant arc it was not involved in the rifting process, but rather became a gradually emergent rift shoulder to the north of the Sumba rift. When volcanic activity was resumed in early Pliocene times, the latest phase of volcaniclastic supply from the sources S of Sumba just had come to an end (late Messinian). This northward return of the eruption centres to approximately their former position strongly suggests a causal relation.

The presence of Miocene volcanoes to the south of Sumba have not been predicted by any of the recent plate tectonic reconstructions of the region (Rangin *et al.* 1990; Daly *et al.* 1991; Hall 1996). Despite the rather different paleogeographic scenarios given by the latter authors, all indicate fundamental changes during the E-M Miocene, due to juxtaposition of the Sunda Arc subduction system with the proto Banda Arc crust. Packham (1996) estimates the age of the Banda Arc > 12 Ma, but not exceeding 15 Ma. According to the Hall (1996) reconstruction of the 15–20 Ma interval, the Sunda Arc was still bent northward along proto Sulawesi to meet the active Sulu system. At 15 Ma sea floor spreading in the South China Sea stopped (Briais *et* al. 1993). Such regional changes in stress patterns, plus the gradual merging with the northward migrating Banda region at approximately the same time, could have been more than a coincidence. In our tentative scenario we propose that around the transition Early-Middle Miocene southeastward trench migration took place S of Sumba, until it could merge eastward with the N-subduction trench as it has existed S of proto-Timor (see maps by Rangin *et al.* 1990; Harris, 1992; Linthout *et al.* 1997). Trench rollback thus may have initiated rifting in the Sumba region. Rifting at that time probably proceeded eastward into the Banda Arc segment. Linthout *et* al. (subm.) provide strong arguments for middle Miocene rifting and ocean floor spreading in the South Banda Arc. Because parts of this oceanic crust have been obducted on N. Timor these relics could represent a more or less lateral equivalent of the rift phase. With Sumba at ~ 12°S in the middle

Miocene, the position of the trench S of Sumba could then have at approximately 13–14°S.

Barberi *et al.* (1987) explained the gap in volcanic activity of the eastern Sunda Arc and its early Pliocene reactivation, by assuming the possibility of acceleration of the subducting plate motion, with concomitant decrease of the slab dip. This seems very plausible in the light of the data of Otsuki (1989).

Conclusions

Study of the Neogene forearc basin sediments on East Sumba and correlation with the offshore seismic record via a synthetic seismogram of Transect II, confirms the working hypothesis that the E Sumba trend of eastward increasing amounts of intercalculated volcaniclastic turbidites continues offshore. On the Sumba Ridge (Fig. 13), the pattern of prograding volcaniclastic turbidites can be traced as far as the Savu Thrust.

The following depositional history is concluded: the angular unconformity between Paleogene platform carbonates and overlying Neogene volcaniclastic submarine fan deposits represents a major break-up stage which resulted in fundamental changes in the middle Miocene outline of the forearc basin. Crustal extension coupled to changes in the process of subduction caused extensive intra-arc rifting with the establishment of a volcanic proto arc to the south of Sumba. Initially subsidence may have exceeded 100 cm/ka, resulting in sediment starvation in parts of the new rift basin. Within the arc-parallel rift basin, NE-SW directed fault zones may have caused a compartmentation. The indications for differential subsidence of the central and east Sumba segments (Fig. 13B), with abyssal environments extending eastward, plus the thickest prograding submarine fans E of Sumba, suggest an eastward increase of rifting.

The onshore Middle-Late Miocene volcaniclastic submarine fan complex up to 600 m thick reveals stacked patterns of shifting fan lobes that partly truncate and partly onlap older sequences. Variation in volcanicity of the hinterland rather than eustatic sealevel fluctuations probably determined the large scale of strata1 patterns. Northward progradation, evident from the offshore seismic profiles is also concluded from the fact that the volcaniclastics of South Sumba (Langhian-early Serravalian) are older than similar basal sequences present N of the Massu mountains. There, volcaniclastic supply was largest in early-middle Tortonian times, waned during the late Tortonian, and was renewed during the Messinian. From the latest Miocene to Recent, uplift took place in East Sumba with an average rate of 70 cm/ka, but faster rates, up to 1 m/ka during the late Pliocene cannot be ruled out.

The paleomagnetic data indicate that during the Neogene, Sumba underwent a slight northward drift and a minor counterclockwise rotation of 5°, which is possibly related to the late Pliocene collision with Australia. The magnetostratigraphic exercise to better constrain the position of the Mio-Pliocene boundary indicates that promising magnetostratigraphic and biostratigraphic correlations can be obtained for the Late Cenozoic of Sumba when undertaken on a larger scale.

The rapid M. Miocene subsidence is probably related to a regional change in the pattern of subduction causing extension in the Sumba region. Prior to this event volcanic activity still took place on Sumbawa and W. Flores. The southward shift of volcanism brought Sumba in a backarc position with regard to a newly created volcanic ridge. Because volcanic activity was resumed in the Sumbawa–Flores sector in the early Pliocene it might be better to speak of an intra arc position of Sumba. The N-S shift of volcanic eruption centres must be related to fundamental changes in subduction configuration. It is tentatively suggested that active subduction, as it existed all around the former Sundaland in the Paleogene, switched during the E-M Miocene eastward due to the arrival of the South Banda region. Rollback of the trench axis S of Sumba occurred, soon merging with the arriving subduction zone S of the Timor terrane. Extension in the Sumba segment may have continued eastward in the South Banda region, where the ocean floor spreading occurred at that time (Linthout *et al.* subm.).

Acknowledgements—This research was carried out under the auspices of LIPI-Geotechnology in Bandung and the Marine Geological Institute (PPGL). Fieldwork on Sumba was possible due to the travel grants from the Netherlands Marine Science Foundation (SOZ). The help of especially T. Priantono, Igna S., S. Hadiwasastra and W. Hantoro during the various field campaigns is gratefully acknowledged. Discussions on various topics with T. B. Roep, T. C. E. van Weering, S. R. Troelstra and K. Linthout were much appreciated. This paper could not have been written without the support of: B. Prins, who kindly shared his great nannofossil skills with us, J. A. M. Kenter, who gave advice and assistance during the preparation of samples for the determination of acoustic properties. whereas J. Stafleu was instrumental in transforming the petrophysical data into synthetic seismogram. Shell International Petroleum Company is acknowledged for providing seismic profile Pac 109. P. Willekes prepared the many samples for micropaleontological investigation. J. E. van Hinte and T. C. E. van Weering provided constructive remarks on the manuscript, which greatly benefitted from editorial comments by A. J. Barber. J. R. Ali, J. Milsom and an anonymous referee. This is contribution Nr. 97104 of the Netherlands Research School of Sedimentary Geology (NSG).

REFERENCES

Adisaputra M. K. (1989) Planktonic foraminfera in recent bottom sediments of the Flores, Lombok and Savu Basins, eastern Indonesia. In Proc. Snellius-II Symposium, part 2, (edited by Van Hinte J. E., van Weering T. C. E. and Fortuin A. R.). *Neth. J. Sea Res. 24,* 465–457.

Audley-Charles M. G. (1985) The Sumba enigma: is Sumba a diapiric forearc nappe in process of formation? *Tectonophysics* **119,** 435-449.

Audley-Charles M. G. (1975) The Sumba fracture: a major discontinuity between eastern and western Indonesia. *Tectonophysics 26, 2* 13- *228.*

Baksi A. K. (1993) A geomagnetic polarity time scale for the period 0-17 Ma, based on 40Ar/39Ar plateau ages for selected field reversals. *Geophys. Res. Lett.* 20, 1607~1610.

Barberi F.. Bigioggero B., Boriani A., Cattaneo M., Cavallin A., Cioni R., Eva C.. Gelmini R., Giorgetti F.. Iaccarino S., Innocenti F.. Marinelli G.. Sleiko D. and Sudratjat A. (1987) The island of Sumbawa: a major structural discontinuity in the Indonesian Arc. *Boll. Soc. Geol. It.* 106, 547–620.

Bartek L. R., Vail P. R., Anderson J. B., Emmet P. A. and Wu S. (1991) Effects of Cenozoic ice sheet fluctuations in Antarctica on the

stratigraphic signature of the Neogene. *J. Geophys. Res.* **96(B4),** 6753 -6778.

Berger W. H., Leckie R. M., Janacek T. R. and Takayama T. (1993) Neogene carbonate sedimentation on Ontong Java Plateau: highlights and open questions. In: *Proc. ODP, Sci. Results.* 130, (edited by Berger W. H., Kroenke L. W.. Mayer L. A., et al.). College Station TX, pp. 71 1–744.

Berger W. H. and Stax R. (1994) Neogene carbonate stratigraphy of Ontong Java Plateau (western equatorial Pacific): three unexpected findings. *Term Nova 6,* 520–534.

Berggren W. A., Kent D. V., Swisher C. C. and Aubry M. P. (1995a) A revised Cenozoic Geochronology and Chronostratigraphy. In *Geochronology, Time Scales and Global Stratigraphic Correlation* (edited by Berggren W. A., Kent D. V. and Hardenbol J.). Soc. Econ. Pal. Min, Spec. Publ. 54, 1299212.

Berggren W. A.. Hilgen F. J., Langereis C. G., Kent D. V., Obradovich J. D., Raffi I., Raymo M. E. and Shackleton N. J. (1995b) Late Neogene Chronology: new perspectives in high resolution stratigraphy. *Geol. Soc. Am. Bull. 107,* 1272–1287.

Blow W. H. (1969) Late Middle Eocene to Recent planktonic foraminiferal biostratigraphy. In: *Proc. Firs/ In/. Conference on Planktonic Microfossils* (1961) pt 1, pp. 199–422.

Bolli H. M., Saunders J. B. and Perch-Nielsen K. (eds) (1995) *Plankton stratigraphy*. Cambridge Earth Sci. Series, Cambridge.

Briais A.. Patriat P. and Tapponnier P. (1993) Updated interpretation of magnetic anomalies and sea floor spreading stages in the South China Sea: implications for the Tertiary tectonics of Southeast Asia. *J. Geoph. Res. 98,* 6299–6328.

Burollet P. F. and Salle C. (1982) Histoire gtologique de l'ile de Sumba (Indonesie). *Bull. Soc. Geol. Fr.. 24,* 573–580.

Cande S. C. and Kent D. V. (1995) Revised calibration of the Geomagnetic Polarity Timescale for the Late Cretaceous and Cenozoic. *J. Geophys. Res.* 100, 6093–6095.

Chaisson W. P. and Leckie R. M. (1993) High resolution Neogene planktonic foraminifera biostratigraphy of Site 806, Ontong-Java Plateau (western equatorial Pacific.) In: *Proc. ODP. Sci Results,* 130, (edited by Berger W. H.. Kroenke L. W., Mayer L. A.. et al.). pp. 1377178.

Chamalaun F. H., Grady A. E., Von der Borch C. C. and Hartono H. M. S. (1982) Banda Arc tectonics: The significance of the Sumba island (Indonesia). Am. *Assoc. Petr. Geol., Mem. 34,* 261–375.

Chamalaun F. H. and Sunata W. (1982) The paleomagnetism of the Western Banda Arc System-Sumba. In: *Paleomagnetic Research in Southeast and East Asia*, Proceedings of a Workshop. Kuala Lumpur. Malaysia, March 1982, CCOP Bangkok. pp. 162–194.

Daly M. C.. Cooper M. A.. Wilson 1.. Smith D. G. and Hooper B. G. D. (1992) Cenozoic plate tectonics and basin evolution in Indonesia. *Mar. Petr. Geol. 8,* 2–2 1.

DeMets C., Gordon R. G., Argus D. F. and Stein F. (1990) Current plate motions. *Geoph. J. In/.* 101, 425478.

De Smet M. E. M., Fortuin A. R., Troelstra S. R., Van Marle L. J.. Karmini M., Tjokrosdpoetro S. and Hadiwasastra S. (1990) Detection of collision-related vertical movements in the outer Banda Arc (Timor, Indonesia). usmg micropaleontological data. *J. SE Asian Earth Sci 4,* 337–356.

Effendi A. C. and Apandi C. (1981) Geological map of Sumba Quadrangle, Nusa Tenggara. Unpubl. map and report, Geol. Res. Dev. Centre Bandung.

Fortuin A. R.. De Smet M. E. M., Hadiwasastra S., Van Marle L. J. and Troelstrd S. R. (1990) Late Cenozoic sedimentary and tectonic history of South Buton, Indonesia. *J. SE Asian Earth Sci. 4,* 107-124.

Fortuin A. R.. Roep Th. B.. Sumosusastro P. A., Van Weering T. C. E. and Van der Werff W. (1992) Slumping and sliding in Miocene and recent developing arc basins, and onshore and offshore Sumba, Indonesia. *Mar. Geol.* 108, 345–363.

Fortuin A. R., Roep Th. B. and Sumosusastro P. A. (1994a) The Neogene sediments of East Sumba, Indonesia–Products of a lost arc? *J. SE Asian Earth Sci. 9, 67-79.*

Fortuin A. R.. Sumosusastro P. A., Berghuis H. W. K. and Roep Th. B. (1994b) Uplifted Pleistocene coral-limestone terraces interfingering with fandeltas and fluviatile conglomerates — a record of sealevel highstands and lowstands between c. 550 and 100 ka (isotopic stages 14 to 5), Waingapu area, Sumba, Indonesia. UNESCO-IUGS Congress Climates of the Past, Den Pasar. Bali, Abstr., p. 15.

Genrich J. F., Bock Y., McCaffrey R., Calais E., Stevens C. and Subarya C. (1996) Accretion of the southern Banda Arc to the Australian plate margin determined by Global Positioning System measurements. *Tectonics*, 15, 288-296.

Hall R. (1996) Reconstructing Cenozoic SE Asia. In: *Tectonic Evolution of* SE *Asia* (edited by Hall R. and Blundell, D. J.). Geol. Soc. of London, Spec. Publ. 106, 1533184.

Hamilton W. (1979) Tectonics of the Indonesian region. U.S. *Geol. Survey Prof. Pop.* 1078, 345 pp.

Hamilton W. (1988) Plate tectonics and island arcs. *Geol. Soc. Am. Bull.* 100, 150331527.

Hantoro W. S. (1992) Etude des Terraces Recifales Quaternaires Soulevees Entre le Detroit de la Sonde et l'Ile de Timor, Indonesie: Mouvements Verticaux de la Croute Terrestre et Variations de Niveau de la Mer. PhD thesis. Univ. Aix-Marseille II. France, vol. I-II, 743 pp.

Haq B. U., Hardenbol J. and Vail P. R. (1988) Mesozoic and Cenozoic chronostratigraphy and cycles of sea-level change. In: *Sea-Level Changes: An Integrated Approach*, (edited by Wilgus C. K.. Hastings B. S., Kendall C. G. St. C., Posamentier H. W., Ross C. A. and Van Wagoner J. C.) Soc. Econ. Pal. Min. Spec. Publ. 42, 71–108.

Harris R. A. (1991) Temporal distribution of strain in the active Banda orogen; a reconciliation of rival hypothesis. *J. SE Asian Earth Sci.* 6, 3733386.

Harris R. A. (1992) Peri-collisional extension and the formation of Oman-type ophiolites in the Banda Arc and Brooks Range. In: *Ophiolites nnd /heir Modern Oceanic Analogues*, (edited by Parson L. M.. Murton B. J. and Browning P.). Geol. Soc. Spec. Publ. 60, 301–325.

Hilgen F. J., Krijgsman W.. Langereis G. C., Lourens L. J., Santarelli A. and Zachariasse W. J. (1995) Extending the astronomical (polarity) timescale into the Miocene. *Earth Plan. Sci. Lett.*, 136, 495-5 10.

Hilgen F. J. and Langereis C. G. (1993) A critical re-evaluation of the Miocene/Pliocene boundary as defined in the Mediterranean. *Earth Plan. Sci. Letts.* 118, 167-I 79.

Ingle J. C. Jr. (1992) Subsidence of the Japan Sea: stratigraphic evidence from ODP sites and onshore sections. In: *Proc. ODP Sci. Results,* (edited by Tdmaki K., Suyehiro K.. Allan J. and McWilliams M. *et al.*), **127/128,** 1197~1218.

Kennett J. P. (1982) *Marine Geology*. Prentice Hall. Englewood Cliffs, 813 pp.

Kenter J. A. M., Podladchikov F. F., Reinders M., Van der Gaast S., Fouke B. W. and Sonnenfeld M. D. (in press) Parameters controlling sonic velocities in a mixed carbonate-siliciclastic Permian shelf-margin (upper San Andres Formation, Last Chance Canyon, New Mexico), *Geophysics*, 62.

Lajoie J. and Stix J. (1992) Volcaniclastic rocks. In: *Facies Models, Response to Sealevel Change*, (edited by Walker R. G. and James N. P.) Geographical Association of Canada, 13, 101–1 19.

Linthout K., Helmers H. and Sopaheluwakan J. (submitted) Late Miocene obduction and micro-plate migration around the southern Banda Sea and the closure of the Indonesian Seaway. *Earth. Plan. Sri. Lett.*

Lourens L. J., Antonarakou A., Hilgen F. J., Van Hoof A. A. M., Vergnaud-Grazzini C. and Zachariasse W. J. (1996) Evaluation of the Plio-Pleistocene astronomical time scale. *Paleoeanography*, 11, 391–413.

Masson D. G., Milsom J., Barber A. J., Sikumbang N. and Dwiyanto B. (1991) Recent tectonics around the island of Timor, eastern Indonesia. *J. Mar. Petr. Geol., 8, 3549.*

Mutti E. (1992) *Turbidite sandstones*. Agip S.p.A, 275 pp.

Mutti E. and Normark W. R. (1987) Comparing examples of modern and ancient turbidite systems: Problems and Concepts. In: *Marine Clastic Sedimentology: Concepts and Case Studies*, (edited by Leggett. J. K. and Zuffa G. G.). Graham and Trotman, 1-38.

Nishimura S., Otofuji Y., Ikeda T., Abe E., Yokoyama T.. Kobayashi Y., Hadiswasastra S., Sopaheluwakan J. and Hehuwat F. (1981) Physical geology of the Sumba, Sumbawa and Flores islands. In: *The Geology and Tectonics of Eastern Indonesia*, (edited by Barber A. J. and Wiryosujono S.). Geol. Res. Dev. Centre. Spec. **Pub].** 2. 103–113.

Dtofuji Y., Sasajima S.. Nishimura S.. Yokoyama T., Hadiwasastra S. and Hehuwat F. (1981) Paleomagnetic evidence for the paleo-position of Sumba island, Indonesia. *Earth. planet. sci. Lett. 52,* 933100.

Otsuki K. (1989) Empirical relationships among the convergence rate of plates, rollback rate of trench axis and island-arc tectonics "laws of convergence rate of plates". *Tectonophysics*, **159, 73-94.**

Packham G. (1996) Cenozoic SE Asia: reconstructing its aggregation and reorganization. In *Tectonic Evolution of SE Asia*, (edited by Hall R. and Bludell D. J.) Geol. Soc. of London, Spec. Publ. 106, 123–152.

Pirazzoli P. A.. Radtke U., Hantoro W. S., Jouannic G., Hoang C. T., Causse C. and Borel Best M. (1993) A one million-year-long sequence of marine terraces on Sumba island, Indonesia. *Marine Geology*, 109, 221–236.

Pitman W. V. and Andrews J. A. (1985) Subsidence and thermal history of small pull-apart basins. In: *Strike-Slip Deformation, Basin Formation, and Sedimentation*, (edited by Biddle K. T. and Christie-Blick N.) Spec. Publ. Soc. Econ. Paleontol. Mineral.. 37, 45549.

Rangin C., Jolivet C., Pubellier M. *et al.* (1990) Paleogeographical and paleokinematic reconstructions; based on close match between geological and kinematic data. Bull. *Soc. Geol. Fr. 6,* 889–905.

Roep T. B. and Fortuin A. R. (1996) A submarine slide scar and channel filled with slide blocks and megarippled *Globigerina* sands of possible contourite origin from the Pliocene of Sumba, Indonesia. *Sedim. Geol.*, 103, 145–160.

Shanmugan G. and Moiola R. J. (1991) Types of Submarine Fan Lobes: Models and Implications. *Am. Assoc. Petr. Geol. Bull. 75,* 156–179.

Snyder D. B.. Prasetyo H., Blundell D. J., Pigram C. J., Barber A. J., Richardson A. and 'Tjokrosapoetro S. (1996) A dual doubly vergent orogen in the Banda Arc continent-arc collision zone as observed on deep seismic reflection profiles. *Tectonics* **15,** 34–53.

Srinivasan M. S. and Kennett J. P. (1981) A review of Neogene planktonic foraminiferal biostratigraphy: applications in the Equatorial and South Pacific. *Soc. Econ. Pal. Min. Spec. Publ., 32,* 395432.

Stafleu J. (1994) Seismic models of outcrops as an aid in seismic interpretation. PhD thesis Vrije Universiteit, Amsterdam, 223 pp.

Stafleu J. and Sonnenfeld M. D. (1994) Seismic models of a shelf-margin depositional sequence upper San Andres Formation, Last Chance Canyon, New Mexico. *J. Sedim. Res.* **B65,** 481–499.

Suga K. and Fujioka H. (1990) Volume of volcanic materials along northern lzu-Bonin Arc. *Volcanological Society of Japan Bulletin* 35, 359–374.

Tjalsma R. C. (1971) Stratigraphy and foraminifera of the Neogene of the eastern Guadalquivir Basin (Southern Spain). *Utrecht Microp. Bull. 4,* 161 pp.

Van Bemmelen R. W. (1949) *The Geology of Indonesia*, Government Printing Office. The Hague, IA. 732 pp.

Van Weering T. C. E.. Kusnida D., Tjokrosapoetro S., Lubis S.. Kridoharto P. and Munadi S. (1989) The seismic structure of the Lombok and Savu forearc basins, Indonesia. *Neth. J. of Sea Res.* 24, 251–262.

Van der Werff W.. Kusnida D., Prasetyo H. and Van Weering T. C. E. (1994a) On the origin of the Sumba forearc basement. *Mar. Prtr. Geol.* **11, 363 314.**

Van der Werf W.. Prasetyo H.. Kusnida D. and Van Weering T. C. E. (1994b) Seismic stratigraphy and Cenozoic evolution of the Lombok Forearc Basin. Eastern Sunda Arc. *Mar. Geol.* **117,** 119–134.

Van der Werff W. (1995a) Seismic stratigraphy and Cenozoic evolution of the Savu forearc basin. forearc response to arc/continent collision. *J. Mar. Petr. Geol.* **12,** 247–262.

Van der Werff W. (1995b) Structure and morphotectonics of the accretionary prism in the eastern Sunda/western Banda Arc. *J. SE Asian Earth Sci.* **11, 309-322.**

Van der Werff W. (I 996) Forearc development and early orogenesis along the eastern Sunda/Western Banda Arc (Indonesia). PhD thesis. Vrije Universiteit, Amsterdam, 31 l pp.

Van der Werff W. (1996) Variation in forearc basin development along the Sunda Arc. Indonesia. *J. S E Asian Earth Sci*, **14,** 331–349.

Veenhof R. (1990) The geology of the Sumba basement. Unpubl. Rept. Inst. of Earth Sciences. Vrije Universiteit, Amsterdam, 44 pp.

Von der Borch C. G., Grady A. E., Hardjoprawiro S., Prasetyo H. and Hadiwasastra S. (1983) Mesozoic and late Tertiary submarine fan sequences and their tectonic significance, Sumba. Indonesia. *Sed. Geol.* 37, I 13–137.

Vroon P. Z., Van Bergen M. J. and Forde E. J. (1996) Pb and Nd isotope constraints on the provenance of tectonically dispersed continental fragments in east Indonesia. In: *Tectonic Evolution of SE Asia.* (edited by Hall R. and Blundell D. J.), Geol. Soc. of London, Spec. Publ. 106, I.

Walker R. G. (1992) Turbidites and Submarine Fans. In: *Facies Models, Response to Sealevel* (edited by Walker R. G. and James N. P.). Geol. Ass. of Canada, 13, 2399263.

Walker G. P. L. (1993) Basaltic-volcano systems. In: *Magmatic Processes and Plate Tectonics*, (edited by Prichard H. M.. Alabaster T., Harris N. B. W. and Neary C. R.) Geological Society of London Special Publ. 76, 3338.

Wensink H. (1994) Paleomagnetism of rocks from Sumba: tectonic implications since the late Cretaceous. *J. S E Asian Earth Sci, 9,* 51–65.

Wensink H. and Van Bergen M. J. (1995) The tectonic emplacement of Sumba in the Sunda-Banda Arc: paleomagnetic and geochemical evidence from the early Miocene Jawila volcanics. *Tectonophysics*, 250, 15–30.

Yamaji A. (1990) Rapid intra-arc rifting in Miocene northeast Japan. *Tectonics, 9,* 365–387.

Zachariasse W. J. (1992) Neogene planktonic foraminifers from Sites 761 and 762 off northwest Australia. In: *Proc. ODP, Sci. Results*, (edited by Von Rad U., Haq B. U. *et al.)* **122, 665-674.**